# Molecular aspects of zygotic embryogenesis in sunflower (*Helianthus annuus* L.): correlation of positive histone marks with *HaWUS* expression and putative link *HaWUS*/*HaL1L*

Mariangela Salvini [1,*,2]

Email m.salvini@sns.it

Marco Fambrini [2]

Lucia Giorgetti [3]

Claudio Pugliesi [2]

[1] Scuola Normale Superiore, Piazza dei Cavalieri 7, 56126 Pisa, Italy

[2] Department of Agriculture, Food and Environment, University of Pisa, Via del Borghetto 80, 56124 Pisa, Italy

[3] Institute of Agricultural Biology and Biotechnology (IBBA), Italian National Research Council (CNR), Via Moruzzi 1, 264100 Pisa, Italy

## Abstract

## *Main conclusion*

**The link HaWUS/*HaL1L*, the opposite transcriptional behavior, and the decrease/increase in positive histone marks bond to both genes suggest an inhibitory effect of *WUS* on *HaL1L* in sunflower zygotic embryos.**

In *Arabidopsis*, a group of transcription factors implicated in the earliest events of embryogenesis is the WUSCHEL-RELATED HOMEOBOX (WOX) protein family including WUSCHEL (WUS) and other 14 WOX protein, some of which contain a conserved WUS-box domain in addition to

the homeodomain. *WUS* transcripts appear very early in embryogenesis, at the 16-cell embryo stage, but gradually become restricted to the center of the developing shoot apical meristem (SAM) primordium and continues to be expressed in cells of the niche/organizing center of SAM and floral meristems to maintain stem cell population. Moreover, *WUS* has decisive roles in the embryonic program presumably promoting the vegetative-to-embryonic transition and/or maintaining the identity of the embryonic stem cells. However, data on the direct interaction between *WUS* and key genes for seed development (as *LEC1* and *L1L*) are not collected. The novelty of this report consists in the characterization of *Helianthus annuus WUS* (*HaWUS*) gene and in its analysis regarding the pattern of the methylated lysine 4 (K4) of the Histone H3 and of the acetylated histone H3 during the zygotic embryo development. Also, a parallel investigation was performed for *HaL1L* gene since two copies of the WUS-binding site (WUSATA), previously identified on *HaL1L* nucleotide sequence, were able to be bound by the HaWUS recombinant protein suggesting a not described effect of HaWUS on *HaL1L* transcription.

**AQ1**

**AQ2**

## Keywords

ChIP
EMSA
In situ hybridization
Gene expression
DNA-binding proteins
NF-Y transcription factor

## Abbreviations

| | |
|---|---|
| ChIP | Chromatin immunoprecipitation |
| DAP | Days after pollination |
| EMSA | Electrophoretic mobility shift assay |
| ISH | In situ hybridization |
| qPCR | Real-time RT-PCR |
| RAM | Root apical meristem |
| SAM | Shoot apical meristem |
| *WOX* | *WUSCHEL-RELATED HOMEOBOX* gene |

Electronic supplementary material

The online version of this article (doi:10.1007/s00425-015-2405-2) contains supplementary material, which is available to authorized users.

# Introduction

The origin of all plants is essentially a simple mature embryo organized with an apical–basal polarity and radial concentric tissue layers perpendicular to the axis of symmetry. At the ends of the axis of polarity, the primary meristems organize: the primary shoot apical meristem (SAM), at the top end, flanked by one or two cotyledons, and the primary root apical meristem (RAM) at the bottom end (~~T~~ten Hove et al. 2015).

Since the early stages of pattern formation and morphogenesis, the stem cell pools, which are essential for the virtually unlimited post-embryonic growth, are specified in the RAM and SAM (Scheres 2007). Conversely, during the following maturation phase, storage reserves accumulate and finally the embryo development arrests (De Smet et al. 2010).

A group of transcription factors (TFs) implicated in the earliest events of embryogenesis is the WUSCHEL-RELATED HOMEOBOX (WOX) protein family. In *Arabidopsis,* this family consists of 15 members: WUSCHEL (WUS) and other 14 WOX proteins, some of which contain a conserved WUS-box and an EAR motif in addition to the homeodomain (Haecker et al. 2004; van der Graaff et al. 2009; Lian et al. 2014). In the egg cell and zygote, *WOX2* and *WOX8* genes are already co-expressed; on the contrary, after the first asymmetric division of the zygote, they are confined in the apical and basal daughter cells, respectively (Haecker et al. 2004). Successively, the functional organization of both meristems depends on *WOX* family members, *WOX5* in the RAM, and *WUS* in the SAM, respectively (Laux et al. 1996; Mayer et al. 1998; Sarkar et al. 2007).

*WUS* transcripts appear very early in embryogenesis, at the 16-cell embryo stage, long before a meristem is evident, and gradually become restricted to the center of the developing SAM primordium (Mayer et al. 1998; Schoof et al. 2000). *WUS* continues to be expressed in cells of the niche/organizing center (OC) of SAM and floral meristems to maintain stem cell population (Laux et al. 1996; Mayer et al. 1998; Lohmann et al. 2001). Also, *WUS* has decisive roles in the embryonic program of *Arabidopsis thaliana* to determine

two cell populations with very different identities: the protoderm and the inner cells (reviewed in ~~T~~ten Hove et al. 2015). To date, it is interesting to note that the relationship between WUS function and master TFs essential to regulate seed development as LEC1-type HAP3 family CCAAT-box binding factors (LEC1 and LEC1-LIKE; Sreenivasulu and Wobus 2013; Hilioti et al. 2014) is poorly investigated. In fact, only one report suggest that WUS-dependent exclusion of LEC1 activity in the putative OC is required in order to fully maintain the embryonic potential in *Arabidopsis* (Zuo et al. 2002).

The protein WUS acts by directly binding to its own specific motifs in more than one hundred of target promoters and preferentially affects the expression of genes with functions in hormone signaling, metabolism, and development (Busch et al. 2010; Zhou et al. 2014). Surprisingly, several data suggest that *WUS* acts as a bifunctional TF (Lohmann et al. 2001; Leibfried et al. 2005; Ikeda et al. 2009).

In a postulated model, that regards the SAM, vegetative stem cell homeostasis is controlled by the interaction between *WUS* and the *CLAVATA* (*CLV*) genes, which are required to rapidly down-regulate *WUS* in apical daughter cells after cell division (Schoof et al. 2000). *WUS* promotes the expression of *CLV3* which, in turn, via activation of the signaling pathway dependent by CLV1/CLV2 protein complex, acts on *WUS* transcription and limits the size of the *WUS*-expressing OC (Brand et al. 2000; Schoof et al. 2000). The ability of the protein WUS to migrate to adjacent cells and activate its own negative regulator is unique to plant stem cell niches (Yadav et al. 2011). A second model, with more complex interactions, regards floral meristems. *WUS* is expressed early during flower development, but is extinguished after that carpel primordia are established (Doerner 2001). This derives in that *WUS* establishes a regulatory loop with its own negative regulator *AGAMOUS* (*AG*), necessary to terminate the maintenance of floral stem cells. It was hypothesized that the suppression of *WUS* activity by *AG* happens in part post-translationally (Lenhard et al. 2001), namely through their respective protein product interaction, because it is still observed when *WUS* is not under control of its own promoter (Doerner 2001). Nevertheless, it was demonstrated that *AG* achieves the temporally precise repression of *WUS* expression through two parallel mechanisms: the direct repression of *WUS* through transcription inhibition, and the transcriptional activation of *KNUCKLES*, which in turn acts to repress *WUS* (Shiraishi et al. 1993; Liu et al. 2011; Sun et al. 2014). Also, *WUS* is under hormonal influence:

cytokinins positively regulate *WUS* expression in the SAM (Kwon et al. 2005; Gordon et al. 2009), but primary SAM initiation and maintenance do not depend on auxin signaling that is implicated in the repression of meristematic features, especially in the context of cotyledon or leaf primordium formation (Furutani et al. 2004; Hay et al. 2004, 2006). However, *WUS* expression during somatic embryogenesis appears to be auxin-dependent (Su et al. 2009).

The tissue specificity of *WUS* transcription seems to involve, in a combinatorial manner, distinct regulatory regions placed in the promoter. In particular, a 57 bp regulatory region is all that is required to control the boundaries of *AtWUS* transcription in the SAM stem cell niche (Bäurle and Laux 2005).

*WUS* regulation can be also subjected to mechanisms usually defined epigenetic (Ptashne 2013a, b; Iwasaki and Paszkowski 2014; Kim and Su 2014; Steffen and Ringrose 2014). Basing on the observation that the gene *AtGCN5*, coding a histone acetyltransferase, is required to control floral meristem through the *WUS/AG* pathway, it has been supposed that the histone acetylation possibly restricts the *WUS* expression domain within the floral meristem turning on a *WUS* repressor (Bertrand et al. 2003). Acetylation, a post-translational modification that affects H3 and H4 histones, is performed by highly specific enzymes identified in both plants and animals (Finley and Copeland 2014). Histone modification system interplays and cross-talks with DNA methylation status that in turn affects the degree and location of histone post-translational modifications (Collings et al. 2013; Rivera et al. 2014). In the promoter region, the methylation of DNA directly lays down the silencing of transcription. In animals, DNA methylation regards cytosines placed in the dinucleotide CpG, but in plants the CpHpG and CpHpHpG patterns can also be involved. DNA methylation, catalyzed by the DNA methyltransferases (DNMTs), can be reversed by the Ten-Eleven Translocation (TET) proteins in mammalian (Wu and Zhang 2010) and the Demeter (Dme) family of DNA glycosylases in plants (Zhu 2009).

In this report, we characterized the gene *WUS* in *Helianthus annuus* (*HaWUS*). Also, we analyze the *status* of the methylated lysine 4 (K4) of the Histone H3 and of the acetylated histone H3 coupled to *HaWUS,* in correlation with *HaWUS* expression pattern during the zygotic embryo development. Then we focus on the putative link between *HaWUS* and *HaL1L* (two copies of the WUS-binding site (WUSATA) were found in the *HaL1L*

nucleotide sequence; Salvini et al. 2012) which can result in an unknown effect of HaWUS on *HaL1L* transcription. In *A. thaliana*, *AtL1L* and its closely related *AtLEC1* encode two peptides which represent the LEC1-type b (or HAP3) subunits of NF-Y TFs. *AtL1L* and *AtLEC1* share a common origin and are both required for the embryogenesis and for the re-acquisition of embryonic competence, but it is not clear if with redundant roles (Lotan et al. 1998; Stone et al. 2001; Kwong et al. 2003; Braybrook and Harada 2008). In the *Helianthus* genus, *HaL1L* mRNA is highly accumulated during both zygotic and somatic embryogenesis (Fambrini et al. 2006). In particular, in epiphyllous plants, *HaL1L* marks the putative founder cells of ectopic embryos (Chiappetta et al. 2009). In sunflower, *HaL1L* is under regulation through DNA methylation and by potential interactions with hormones and TFs (Salvini et al. 2012).

# Materials and methods

## Plant material and growth condition

Sunflower plants (*Helianthus annuus* L.) from the inbred line HOR were grown in field conditions (Experimental fields, University of Pisa, Pisa, Italy). Plant growth conditions were as previously described (Berti et al. 2005). Briefly, progenies were grown using 50 cm inter-row spacing with 25–30 cm between plants (about 8–9 plants $m^{-2}$).

## Isolation of the *HaWUS* gene and its flanking 5′- and 3′-region

Genomic DNA was extracted from young leaf blades of 25–30-day-old plants with the Nucleon DNA extraction and purification protocol for plant tissue (GE Healthcare Europe, UK), according to the manufacturer's instructions. Sequence information from the previously characterized *HaWUS* cDNA was used to isolate by PCR the intron/exon region of *HaWUS* (Salvini et al. 2012). *HaWUS*-specific primers WUS1F (Supplemental Table S1 and Supplemental Fig. S1) (located 66 nucleotides upstream from the ATG) and WUS2R (Supplemental Table S1 and Supplemental Fig. S1) (located 90 nucleotides downstream from the translational stop codon) were used. The PCR conditions were 94 °C for 4 min, 35 amplification cycles (30 s at 94 °C, 30 s at 58 °C, 1 min 40 s at 72 °C), and a final extension of 7 min at 72 °C.

Genome Walker DNA walking was used to find genomic DNA sequences adjacent to the 5′- and 3′-region of the *HaL1L* gene (Siebert et al. 1995). For

the 5′ RAGE, genomic DNA was digested with *Ale*I restriction enzyme and ligated to Genome Walker Adaptor, according to the manufacturer's instructions (Clontech-Takara Bio Inc., Otsu, Japan). The first PCR was conducted with the AP1 primer provided in the kit and the *HaWUS*-specific primer WUSRAGE1 (Supplemental Table S1). The nested PCR was conducted with the nested adaptor primer (AP2) and the nested *HaWUS*-specific primer WUS15R (Supplemental Table S1). For the 3′ RAGE, genomic DNA was digested with *Ale*I restriction enzyme and attached to Genome Walker Adaptor, according to the manufacturer's instructions (Clontech-Takara). The first PCR was conducted with the AP1 primer provided in the kit and the *HaWUS*-specific primer WUS3WALK1 (Supplemental Table S1). The nested PCR was conducted with the nested adaptor primers AP2 and the nested *HaWUS*-specific primer WUS3WALK2 (Supplemental Table S1). The PCRs were conducted in conditions recommended by manufacturer (Clontech-Takara).

All PCR products were separated by electrophoresis on a 1.5 % TAE agarose gel and visualized with ethidium bromide under UV light. Selected amplified products were purified using the Wizard® SV Gel and PCR Clean-UP System (Promega Corporation, Madison, WI, USA), inserted into the pGEM-T Vector (Promega), and transformed in *Escherichia coli* JM109 competent cells (Promega). Plasmid DNA was prepared using Wizard® *Plus* Minipreps DNA Purification Kit (Promega). Several clones were automatically sequenced on both strands by MWG Eurofin Operon (Ebersberg, Germany). Sequence data were deposited in GenBank under the following accession number LN811433.

## In silico analysis

The genomic sequence was analyzed by the following software: GENESCAN available at http://www.mobyle.pasteur.fr/cgi-bin/portal.py?form=genescan; FASTA, BLAST, and CLUSTALW available sites http://www.ebi.ac.uk/ and http://www.ncbi.nlm.nih.gov/; TSSP at the site http://molbiol-tools.ca /Promoters.htm. The intron, as well as upstream and downstream regions of the *HaWUS* gene was searched for putative TF-binding sites using TRANSFAC (Transcription Factor Binding Sites Database) (Wingender et al. 2001) (http://www.gene-regulation.com/) and MatInspector, which utilizes the PLACE database for plants cis-elements (http://www.genomatix.de/cgi-bin /eldorado/main.pl). The upstream region was searched for putative promoter sequence using the PromoterInspector software available at http://www.genomatix.de/cgi-bin/eldorado/main.pl. (Cartharius et al. 2005)

PROMO, available at http://alggen.lsi.upc.es/cgi-bin/promo_v3/promo/promoinit.cgi?dirDB=TF_8.3, was also used to detect putative TF target sites (Messeguer et al. 2002; Farré et al. 2003).

## Database search and phylogenetic analysis

Database searches were carried out using the BLAST program at the National Center for Biotechnology Information (NCBI) (Altschul et al. 1997); moreover, PROSITE and PFAM databases were searched to identify conserved domains (Bateman et al. 2002; Falquet et al. 2002) (Supplemental Fig. S2). Alignment was performed with the BLOSUM matrix using the ClustalW algorithm-based AlignX module from Mega4. Phylogenetic relationships were calculated using UPGMA (Unweighted Pair Group Method with Arithmetic Mean) (Sneath and Sokal 1973) and bootstrap values with 100 replicates were determined using the Mega4 package (Tamura et al. 2007). The predicted protein sequences used to generate the tree are listed in the caption of Fig. 3.

## Modeling the three-dimensional structure (3D) of WUS domain

The HLH region of HaWUS was identified based on the known structures of from other species (Supplemental Fig. S2) Additionally, the entire sequence was subjected to GENO3D (Combet et al. 2002) and the model pdb2m0cA was chosen in the template analysis for protein conformational sampling (Supplemental Fig. S3). The algorithm is freely accessible at http://geno3d-pbil.ibcp.fr. The ten possible structures returned as output files were displayed by Deep View/Swiss Pdb-viewer (4.1 version) available at http://www.expasy.org/spdbv/ (Guex and Peitsch 1997).

## Construction of digoxigenin-RNA probes

For probes, a 712 bp *HaWUS* fragment was amplified with gene-specific primers WUSPE, and WUSRESP (Supplemental Table S1), while a 676 bp *HaKNOT2* fragment, of a class I *KNOX* gene (GenBank accession number AM991290.1), was amplified with gene-specific primers KNOT2F, and KNOT2R (Supplemental Table S1). In the PCR amplifications, cDNAs were used as template. The fragments obtained were cloned into pGEM® -T easy vector (Promega). Plasmid DNA was prepared using Wizard® *Plus* Minipreps DNA Purification Kit (Promega). Selected clones were automatically sequenced on both strands and then they were used as template to synthesize

digoxigenin (DIG)-labeled RNA sense and antisense probes, according to the DIG-RNA Labeling Kit protocol (Roche).

## In situ hybridization

From the inbred line HOR, zygotic embryos at 10 and 26 days after pollination (DAP), and vegetative shoots (VS) of 25–30-day-old plants were excised and fixed in *p*-formaldehyde. The materials were dehydrated, paraffin embedded, cut into 8 μm sections, and hybridized at 45 °C overnight to DIG-labeled *HaWUS* and *HaKNOT2* RNA probes according to Jackson (1991). For immunological detection, the slides were processed according to Chiappetta et al. (2009). Accumulation of *HaWUS* and *HaKNOT2* transcripts was visualized as a violet/brownish stain.

## Gene expression analysis by real-time RT-PCR (qPCR)

*Helianthus annuus* total RNA was extracted from zygotic embryos collected at 5, 13, and 30 days after pollination (DAP) and mature leaves (15 cm long) of 60-day-old plants. Extraction was performed using the TriPure Isolation Reagent, according to the manufacturer's instructions (Roche). The RNA integrity was controlled by gel electrophoresis and treated with RNase-Free DNase (Life technologies, Thermo Fisher Scientific Inc.) following the manufacturer's instructions. The *HaWUS* cDNA nucleotide sequence is available in nucleotide database at EMBL with the accession number HE616565 (Salvini et al. 2012).

Real-time quantitative qPCRs were performed using a Real-time Step One (Applied Biosystem, Thermo Fisher Scientific Inc, USA) and gene-specific primers for *HaL1L*, *HaWUS,* and *HaACT2*. Quantitative PCR was performed using 20 ng of cDNA and Power SYBR Green RNA-to-Ct 1 Step Kit (Applied Biosystem, Thermo Fisher Scientific Inc. USA, cat. Num. 4389986), according to the manufacturer's instructions. The thermal cycling conditions of RT-PCR were as follows: Reverse transcription: 48 °C-30′; Activation: 95 °C-10′; Cycling: 40 cycles 95 °C-15′/60 °C-30′; Melt curve: 95 °C-15″/60 °C-15″/95 °C-15″. Relative quantification of specific mRNA levels was performed using the comparative $2^{-\Delta(\Delta C_t)}$ $2^{-\Delta\Delta C_T}$ method (Livak and Schmittgen 2001). Expression values were normalized using the housekeeping gene *HaACT2* mRNA, encoding a β-actin (ACT2) (GenBank accession number FJ487621.1) and leaf mRNAs were used as reference sample. The primers used to amplify *HaACT2* cDNA were QACTF and

QACTR. Primers used to amplify *HaWUS* cDNA were QWUSF and QWUSR. Primers used to amplify *HaL1L* cDNA were QL1LF and QL1LR (Supplemental Table S1).

## Electrophoretic mobility shift assay (EMSA)

The EMSAs were performed according to protocols described in Salvini et al. (2012), and here briefly summarized. Firstly, an analysis of the amino acid sequence, deduced from *HaL1L* cDNA, was performed by PROSO II software (http://mips.helmholtz-muenchen.de/prosoII/prosoII.seam), and PredictProtein software (https://www.predictprotein.org/). This approach allowed choosing a fragment of 122 aa, at protein N-terminal tail, that contains the DNA-binding domain and is soluble in a wheat germ *cell-free* protein system for the in vitro transcription–translation. A linear DNA template construct, coding the above protein fragment, was produced with the RTS Wheat Germ LinTempGenSet (5 PRIME, Hamburg, Germany). All the necessary PCRs were performed using the ExpandTM High Fidelity PCR System (Roche). Successively, the DNA template construct was used for the recombinant protein synthesis in an in vitro eukaryotic *cell-free* protein synthesis system based on a wheat germ lysate, the RTSTM Wheat Germ Continuous Exchange *Cell-Free* (CECF) in vitro protein expression reactions (5 PRIME). The 6His-tagged WUS recombinant protein was purified under native conditions by PerfectPro Ni–NTA Agarose (5 PRIME) and employed in EMSAs that were performed with DIG-labeled synthetic double-strand oligonucleotides 39 bp long, as probes, according to DIG Gel Shift Kit, 2nd generation (Roche) protocol. The DIG-labeled probes were prepared starting from 39 mer single-strand sense oligonucleotides, named EMSA3 and EMSA6 along with their complementary antisenses, corresponding to the *HaL1L* intron and 5′ upstream region, near the CG riche isle (IS1) analyzed as regards DNA methylation (Salvini et al. 2012), respectively, and containing the WUSATA motif (according to Bao et al. 2004). The sequence of EMSA3 sense was 5′-CACGTTTGATACGCGATATTAAAAAATGAGTTGAGAGA-3′, and of EMSA6 sense was 5′-TATGTATATATGATGTCATTAATATGATGTTATATATTC-3′, where the WUSATA motifs, in the two opposite orientation, are underlined. The oligonucleotides were purchased from Eurofin MWG Operon. Unlike with what is described in Salvini et al. (2012), the reaction mixtures were loaded onto a 2 % agarose gel in 0.5× TBE buffer. The gel was pre-run (10 min) and run at 50 V/cm. Loading buffer without bromophenol blue was added to the samples, meanwhile loading buffer with bromophenol blue was loaded in an

empty lane of the gel to follow the run. After the run, the gel content was transferred to a positively charged membrane (Roche) by capillarity. Finally, chemiluminescent detection was conducted as described in the DIG Gel Shift Kit (Roche) procedure to make visible the protein/probe complex.

## Chromatin immunoprecipitation (ChIP)

The ChIP protocol, substantially according to Lawrence et al. (2004), and the utilized solutions are exhaustively described in Supplemental Materials and methods. In brief, ChIPs were performed starting from isolated nuclei of embryos at 13 and 30 DAP, and from mature leaves (data not shown). The chromatin (Ch), with cross-linked proteins, was extracted and fragmented by sonication to an average fragment size of 400–500 bp. The Ch was immunoprecipitated with anti-acetyl histone H3 rabbit polyclonal antibodies (MILLIPORE ChIP grade, cat. 06-599, 1 mg/ml). The employed immunogen is a linear peptide corresponding to human histone H3 acetylated at the N-terminus. Also, anti-trimethyl K4 histone H3 rabbit polyclonal antibodies (ABcam ChIP grade, ab8580, 1 mg/ml) were used. The immunogen was a synthetic peptide corresponding to the first 100 amino acids of human histone H3 containing K4me3. As shown in the alignment of the H3 protein sequences of human origin, plants (e.g., *H. annuus*) and protozoan (Supplemental Fig. S4), the amino acids are highly conserved, in particular as regards the Ks, which can be acetylated, and the K4 which can be methylated; so we decided that the above-mentioned antibodies are capable of specifically interacting with *H. annuus* histone H3. Also, the utilized ABcam and Millipore products were found used in several analogous published studies (e.g., ~~Chenlong~~Li et al. 2009; Zheng et al. 2014). Moreover, polyclonal IgGs (ab27478), purified from serum collected from a rabbit prior to immunization, were utilized as a control for non-specific interactions (examples of signals relative to non-specific products are shown in Supplemental Fig. S5 and Supplemental Fig S6). Finally, as a quality control for successful ChIP, negative and positive controls were performed by PCRs, that confirm the absence of amplification products corresponding to a fragment (698 bp) of the CACTA transposable element *Tetu1* (Fambrini et al. 2011; Supplemental Fig. S7), and the presence in the ChIP samples of the housekeeping genes *HaACT2*, amplified with QACTF and QACTR (Supplemental Fig. S8), or pyruvate phosphate dikinase (PYR) (DH0AG10ZA12RM1, *A. thaliana* putative orthologue At4g15530), amplified with PYRF and PYRR (Hewezi et al. 2006) (Supplemental Table S1).

## qPCR on ChIP material

The used apparatus for qPCR was Real-time Step One (Applied Biosystem, Thermo Fisher Scientific Inc., USA). The qPCR run method was: Holding stage 95°-15″/Cycling stage: 40 cycles at 95° for 15″/Melt curve stage 95°-15″/60°-1′/95°-15″ (0.3 increment).The kit used was FAST SYBR Green (Applied Biosystem, Thermo Fisher Scientific Inc USA, c.n. 4385612). The primer combinations were Is1-L1LF, Is1-L1LR; TATA-L1LF, TATA-L1LR; L1L-3ENDF, L1L-3ENDR for *HaL1L*; TATA-WUSF, TATA-WUSR; 3END-WUSF, 3END-WUSF for *HaWUS* (Supplemental Table S1 and Supplemental Fig. S9).

Relative quantification of specific DNA levels was performed using the comparative-$2^{-\Delta(\Delta C_t)}$ $2^{-\Delta\Delta C_T}$ method (Livak and Schmittgen 2001). The Input Method was used as this includes normalization in the respect of INPUT SAMPLEs that represent the starting amount of chromatin used in the ChIP. The data were also normalized in the respect of housekeeping genes *HaACT2* (Hewezi et al. 2006) (Supplemental Table S1), according to Perrella et al. 2013. The data were correct for dilutions subtracting the opportune values from the sample Ct values, so for the input fraction, that was usually used as a 1 % dilution of the starting sample, 6.644 cycles (i.e., $\log_2$ of 100) had to be subtracted.

## Statistical analysis

In each experiment, the values displayed on graphs are means (±SD) from three independent qPCR analyses with 3–4 different RNA or ChIP replicates for each embryo phase or for leaf. All qPCR analyses were performed with three different replicates in each run for all biological samples. Data were treated using ANOVA test (ANalysis Of VAriance between groups) available at http://www.physics.csbsju.edu/stats/anova.html, and means were compared by Tukey's test available at http://faculty.vassar.edu/lowry/hsd.html.

# Results

## Organization of genomic DNA region containing *HaWUS*

We had already isolated a cDNA relative to *HaWUS* containing the entire coding region (CDS), the 3′ end, until the poly(A) tail and a 5′ border fragment (Salvini et al. 2012). Information, derived from the cDNA nucleotide sequence, has been used to sequence and analyze a genomic DNA

fragment containing the entire *HaWUS* gene. A first portion consisting in the full-length intron/exon region (comprehensive of three exons and two introns) 1046 bp in length has been amplified by PCR with the WUS1F/WUS2R primers (Fig. 1 and Supplementary Fig. S1). The positions of introns have been deduced by comparing *HaWUS* cDNA (Salvini et al. 2012) with the genomic DNA sequence. The introns (239 and 565 bp, respectively) had recognizable canonical GT/AG borders. Next, genomic DNA walking has been used to isolate the flanking regions of the *HaWUS* gene (Supplementary Fig. S1). Amplified products, 3586 bp long, have been cloned and sequenced. They have been found to extend 703 bp to the 5′ end and 2962 bp toward the 3′ end, respectively, when the putative *HaWUS* transcription start site (TSS) has been chosen as the start nucleotide for sequence numeration (−1/+ 1). The promoter region of *HaWUS* has been located by TSSP, available at the site http://www.sofberry.com/, basing the search on the consensus sequences that in plants characterize regions flanking the coding sequence. The TSS has been identified in the CA dimer, where the adenine residue represents the first transcribed nucleotide (Fig. 1a, b; Supplementary Fig. S1). The Y<u>R</u>-rule (where TSS is R underlined, Y stands for C or T and R stands for A or G) is respected as many as 77 % of the *Arabidopsis* promoters. Also, a Initiator motif (Inr) is visible surrounding the TSS: YY<u>A</u>NYY, where TSS is underlined, and Y = C/T; N = any base. The *HaWUS* promoter is of the ‘TATA type’ for the sequence TTATA found at -33 bp before the TSS (Fig. 1a, b; Supplementary Fig. S1). A CC dimer, upstream of TATA box and specific to plants, and a Y-Patch motif (CTCCCT) contiguous to TSS at its 5′ side are also present (Fig. 1a, b; Fig. S1).

**Fig. 1**

Schematic representation of the *WUSCHEL* gene of *Helianthus annuus* (*HaWUS*). The GenBank accession number is LN811433. **a** The *light blue rectangle* indicates the promoter region of *HaWUS*. The CCAAT target sequence for NF-Y is in red characters. CA indicates the putative *HaWUS* transcription start site (TSS) as well as the start of nucleotide sequence numeration (−1/+1). ATG and TAATGA represent the *HaWUS* translation start and stop codons, respectively. The *green rectangles* represent the three exons of *HaWUS* joined by two introns depicted as *lines*. The *orange rectangle* represents the 3′-region of *HaWUS*. The transcript cut site (TA) is shown in *light blue*. **b** The nucleotide sequence of the *HaWUS* proximal promoter. The TATA Box is written in *italic* and *bold* characters. The CC dimer, upstream of the TATA box and specific for plants, is in *red* characters. CA, the putative HaWUS transcription start site (TSS) and start nucleotide sequence numeration

(−1/+1), is *underlined*. The Y-Patch, specific to proximal plant promoters, is *boxed*. The ATG is written in *bold* and *green* characters

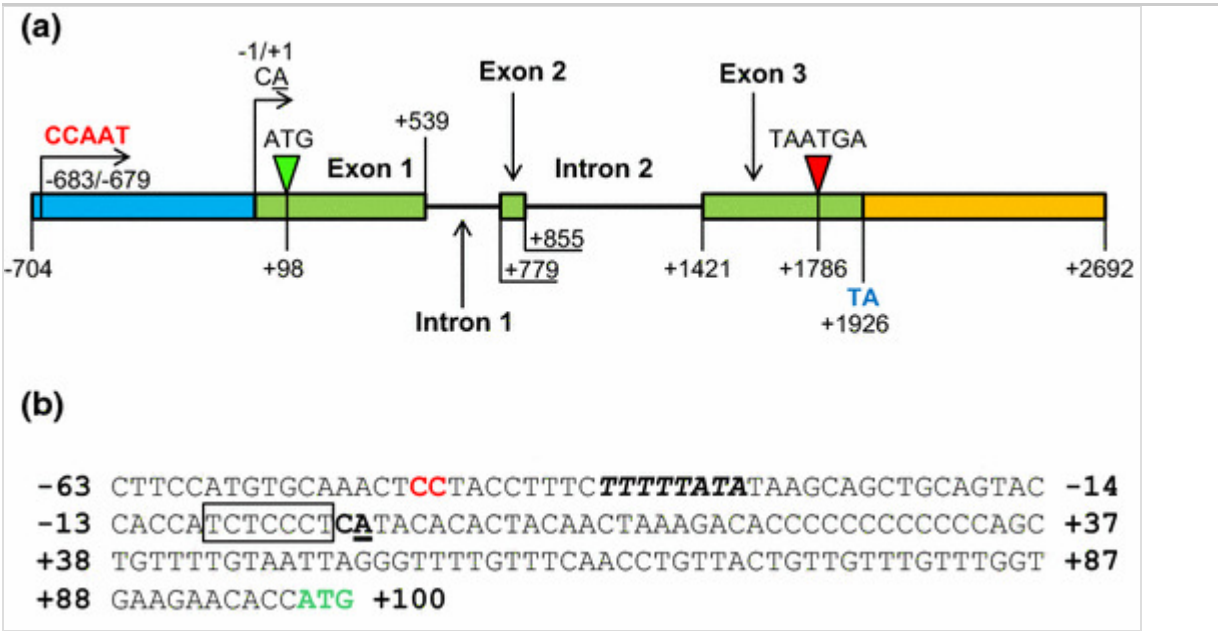


## A survey of the amino acid sequence of HaWUS and a 3D modeling of its WOX domain

The coded protein, deduced from the nucleotide sequence of the *HaWUS* genomic DNA, has been compared with the amino acid sequences of WUS and WOX family proteins of *A. thaliana* (Supplemental Fig. S2). The WOX domain (from T28 to K89), the WUS-box (from T236 to H243) and the EAR-like motif (from L281 to L286) have been identified in HaWUS, according, with minor differences, to Haecker et al. (2004), van der Graaff et al. (2009), Ikeda et al. (2009), and Lian et al. (2014). Also, an acidic region from E216 to E229 is conserved in HaWUS in the respect to the fragment L234–A247 of AtWUS (Ikeda et al. (2009). In particular, as regards the WOX domain, the helix-turn-helix (HTH) motif of pfam00046 family has been recognized, both by searching into the Conserved Domain Database (CDD) at NCBI (http://www.ncbi.nlm.nih.gov) and by the program InterPro at EMBL-EBI (http://www.ebi.ac.uk/). The HTH motif is typical of the homeobox domain, or homeodomain (IPR001356 in InterPro), and it is characterized, in the simplest form, by two alpha-helices, joined by a short turn (Rosinski and Atchley 1999). A HTH motif, in tri-helical form, spanning from T32 and R87, has also been built in the 3D structure of the HaWUS WOX domain (Supplemental Fig. S3) by an in silico analysis with GENO3D algorithm (http://geno3d-pbil.ibcp.fr) (Combet et al. 2002). Moreover, the HTH motif resulted actually able to bind the WUSATA motives placed both in

the promoter and in the intron of *HaL1L*, as demonstrated by EMSAs performed with a WUS recombinant protein containing the fragment T32-R87 (see the section below dedicated to EMSAs and Salvini et al. 2012).

A phylogenetic analysis was performed employing a data set including some of the published amino acid sequences of WUS of other species and the *A. thaliana* WOX family. The resulting UPGMA phylogenetic tree confirms that the HaWUS belongs to the WUS protein subgroup well separated, with a 100 bootstraps value, from the WOX protein subgroup (Fig. 2).

**Fig. 2**

Phylogenetic tree obtained with the UPGMA method. The relationships between 9 WUS proteins including HaWUS and the *A. thaliana* WOX family are shown. The consensus radial tree was inferred by UPGMA (Unweighted Pair Group Method with Arithmetic Mean), with 100 as bootstrap replicates, using Mega4 software (Tamura et al. 2007). HaWUS: *Helianthus annuus* WUS, GenBank accession HE616565.1; AtWUS: *Arabidopsis thaliana* WUS, GenBank accession NM_127349; GmWUS: *Glycine max* WUS, GenBank accession. XP_003517180; NsWUS: *Nicotiana sylvestris* WUS, GenBank accession. XP_009792214; StWUS: *Solanum tuberosum* WUS, GenBank accession XP_006340731; MtWUS: *Medicago truncatula* WUS, GenBank accession XP_003612158; MdWUS: *Malus domestica* WUS, GenBank accession XP_008337592; SlWUS: *Solanum lycopersicum* WUS, GenBank accession ADZ13564; AmWUS: *Antirrhinum majus* WUS, GenBank accession Q6YBV1; AtWOX1: *A. thaliana* WOX1, GenBank accession AY251394; AtWOX2: *A. thaliana* WOX2, GenBank accession NM_125325; AtWOX3: *A. thaliana* WOX3, GenBank accession NM_128422; AtWOX4: *A. thaliana* WOX4, GenBank accession FJ440850; AtWOX5: *A. thaliana* WOX5, GenBank accession AY251398; AtWOX6: *A. thaliana* WOX6, GenBank accession AY251399; AtWOX7: *A. thaliana* WOX7, GenBank accession NM_120659; AtWOX8: *A. thaliana* WOX8, GenBank accession AY251400; AtWOX9: *A. thaliana* WOX9, GenBank accession AY251401; AtWOX10: *A. thaliana* WOX10, GenBank accession NM_101923; AtWOX11: *A. thaliana* WOX11, GenBank accession AY251402; AtWOX12: *A. thaliana* WOX12, GenBank accession AY251403; AtWOX13: *A. thaliana* WOX13, GenBank accession AY251404; AtWOX14: *A. thaliana* WOX14, GenBank accession NM_101922. *Scale bar* represents the number of amino acid substitutions per site. As support for the tree, the bootstrap value at the node, separating the WUS proteins from the WOX proteins, is 100

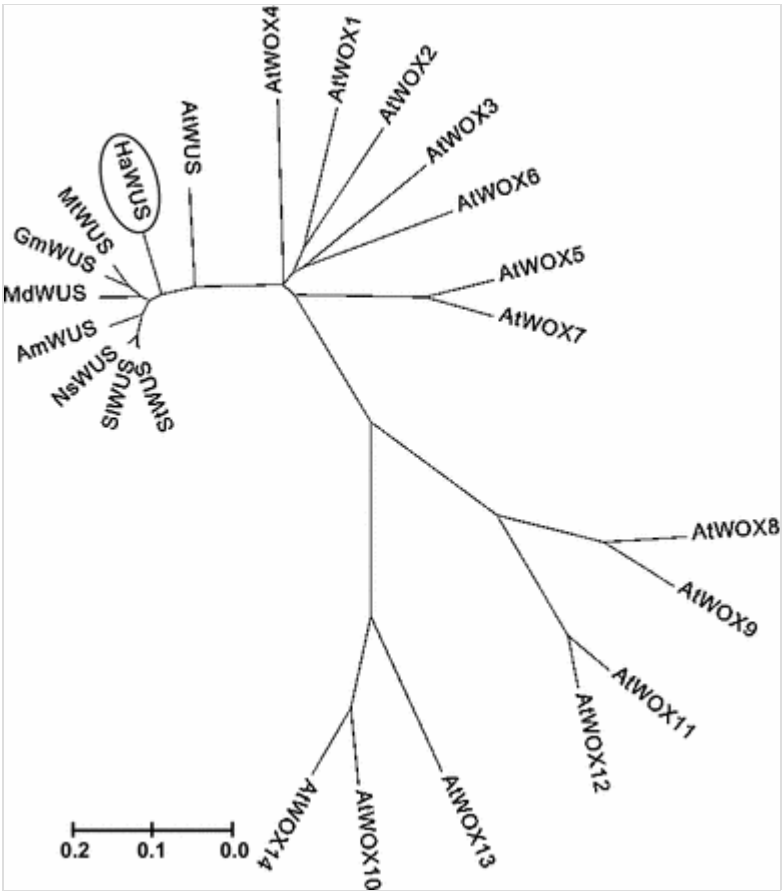


## HaWUS can bind WUSATA motif on *HAL1L* promoter

To obtain more information about the putative action of the TF HaWUS on the expression of *HaL1L* (Salvini et al. 2012), we extended the analyses of the recombinant WUS protein ability to binding the WUSATA motifs placed near the Isle1 (IS1) in the *HaL1L* promoter (according to Bao et al. 2004). IS1 is a region of particular interest being subject to variations in the pattern of DNA methylation during embryonic development of sunflower (Salvini et al., 2012). An EMSA was performed according to Salvini et al. (2012), with a recombinant WUS protein that coincides with the amino terminus of the protein and contains the DNA-binding domain. The employed probe consisted in a 39 mer single-strand oligonucleotide identical to the *HaL1L* nucleotide sequence carrying the WUSATA motif and placed near IS1.

We found that the recombinant WUS protein was able to bind and slow down the probe, as the protein/probe complex was electrophoretically delayed in comparison to the free probe (Fig. 3: lanes 2 and 1, respectively). The binding specificity was proved by the ability of an excess of unlabeled probe to remove the labeled probe from the complex with the recombinant WUS protein (Fig. 3: lane 3). As a control of the EMSA procedure, an analogous analysis regarding the WUSATA motif located in the *HaL1L* intron was

performed as already described in Salvini et al. 2012 (Fig. 3: lanes 4, 5 and 6).

**Fig. 3**

HaWUS binds to *HaL1L* in the IS1-5′ and the intron regions. Immunodetection of EMSA performed with recombinant WUS (RW). *Lane 1, 4* free probes consisting in DIG-labeled 39 ds oligonucleotides containing the WUS-binding motif. *Lane 2, 5* RW/probe complexes delayed in comparison to the free probes. *Lane 3*, *6* the probes are removed from the complexes with RW by the unlabeled 39 ds oligonucleotides. *Lanes 1, 2*, and *3* are referred to IS1-5′ region; *lanes 4, 5*, and *6* are referred to the intron region. For a description of the construct containing a recombinant WUS protein fragment, see Fig. 5 in Salvini et al. 2012

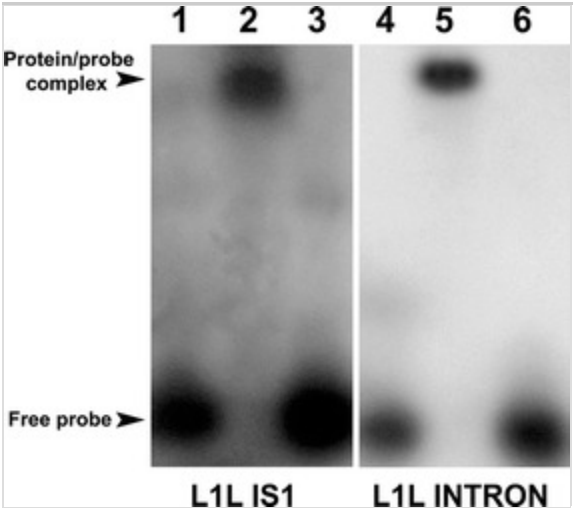


## *HaWUS* transcript localization

In situ hybridization on sections of sunflower zygotic embryos at 10 and 26 DAP revealed that *HaWUS* marks few cells in the shoot apical meristems (SAMs) (Fig. 4a, c). No transcription was detected with the sense RNA probes (Fig. 4b, d). In non-meristematic cells of 26 DAP embryos, a non-specific staining was detected (Fig. 4e). It could be related to the high accumulation of oil bodies in this developmental phase and/or to the long incubation with NBT requested for the hybridisation signal detection (DIG Application Manual for Nonradioactive In Situ Hybridization 4th Edition, Roche, 2008). In situ hybridization on sections of sunflower SAMs demonstrated that *HaWUS* RNA accumulates in small group of cells in the center of the SAM underneath the outermost cell layers of the meristem (Fig. 5a, b). This expression pattern is consistent with the results observed in zygotic embryos and post-embryonic tissues of *A. thaliana* (Mayer et al.

1998). In longitudinal sections of SAMs, a class 1 *KNOTTED*-like gene of sunflower *HaKNOX2* transcripts was strongly detected in the meristematic dome, while incipient leaf primordia were lacking of signal (Fig. 5c). No transcription was detected with the sense RNA probes of both genes (Fig. 5d, e).

**Fig. 4**

Patterns of ~~transcript localization of *HaWUS* and~~*HaWUS* transcript localization in sunflower (*Helianthus annuus*) embryos of 10 (**a**) and 26 (**b**) days from pollination (DAP) in the inbred line HOR. In longitudinal sections of embryos, hybridized with antisense *HaWUS* probe, RNA accumulation is detected in a small domain in the center of the shoot apical meristem (*arrows*). **c**, **d** Longitudinal section of 10 and 26 DAP embryos hybridized with sense probe from *HaWUS*, respectively. Note the absence of hybridization signal in the regions corresponding to the RNA accumulation detected in **a** and **b**. **e** A closer view of cotyledonary cells of 26 DAP embryos (**b**) characterized by non-specific staining. The same signal was detected in cotyledonary cells of 26 DAP hybridized with a sense probe (**d**). *Bars* 170 μm in **a**, 280 μm in **b**, 175 μm in **c**, 260 μm in **d**, and 31 μm in **e**

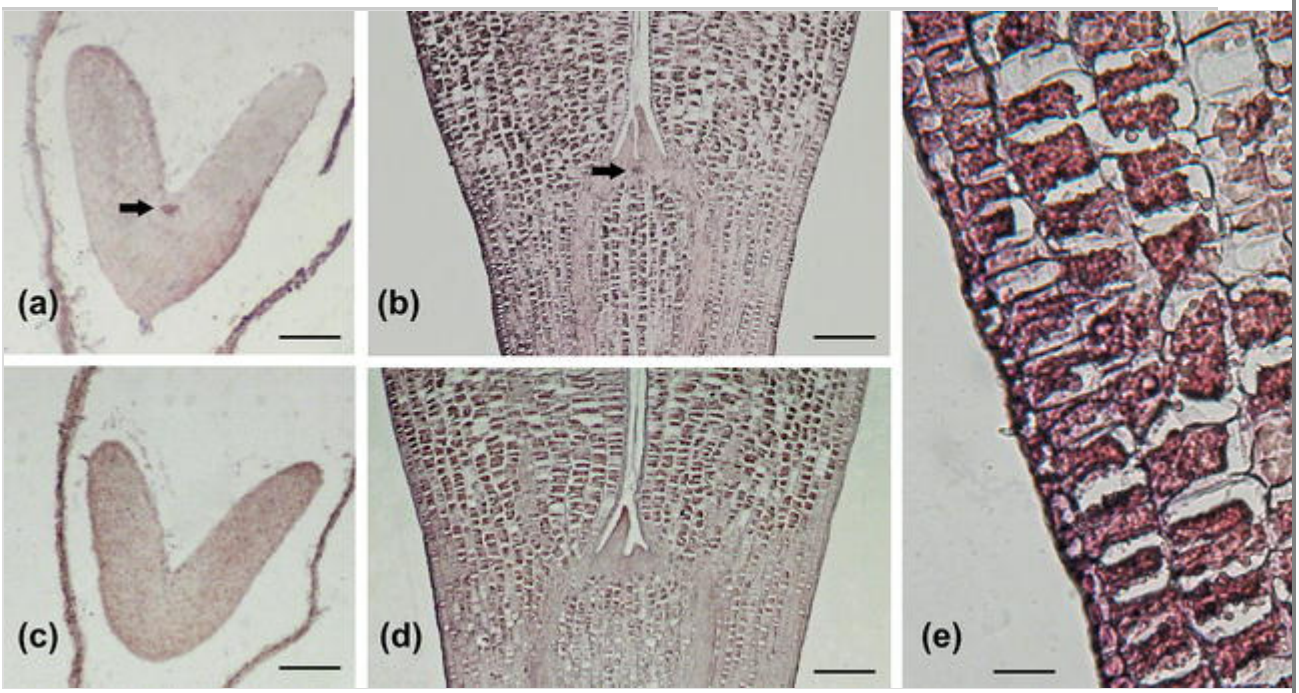


**Fig. 5**

Patterns of ~~transcript~~ localization of *HaWUS* and *HaKNOT2* transcripts in sunflower (*Helianthus annuus*) vegetative shoot apical meristems (VS) of a 25–30-day-old plants in the inbred line HOR. **a**, **b** Longitudinal sections of VS hybridized with antisense probe from *HaWUS*. RNA accumulation is detected in

a small domain in the center of the meristem (*arrowheads*). **c** Longitudinal section of a VS hybridized with antisense probe from *Ha-KNOT2* (GenBank accession number AM991290.1). **d**, **e** Longitudinal section of VS hybridized with sense probe from *HaWUS* and *HaKNOT2*, respectively. *Bars* 80 μm in **a**, 110 μm in **b**, 200 μm in **c**, 270 μm in **d**, and 220 μm in **e**

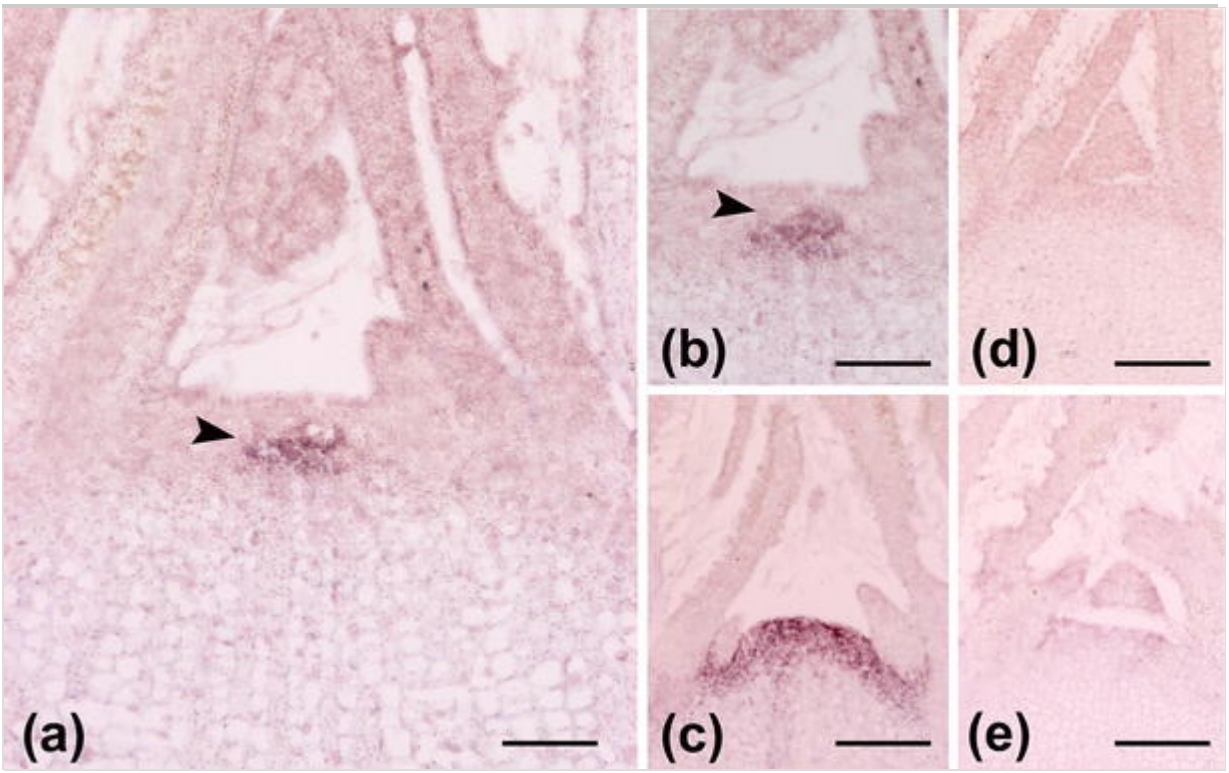


## Putative target sites of regulatory proteins are located throughout the *HaWUS* sequence

A typical putative target sites for NF-Y TF are easily recognizable in the CCAAT sequence, localized at -682 bp from TSS. Also, putative target sites of both positive and negative regulatory proteins have been found scattered throughout the *HaWUS* genomic sequences by the MatInspector software (Cartharius et al. 2005). Sites with matrix similarity 0.9 are shown in Supplemental Figs. S10, S11, S12, and S13. Other putative target sites that were detected by the software PROMO (Messeguer et al. 2002; Farré et al. 2003) are discussed.

## Gene expression analysis by qPCR

To inspect the expressions of *HaWUS* and *HaL1L* during embryo development, an analysis of the steady-state mRNAs has been performed in 5, 13, and 30 DAP embryos for both genes (Fig. 6). The mRNAs coding the two TFs display an opposite behavior, and the amount of *HaWUS* mRNA remains

essentially the same from 5 to 13 DAP, but increases significantly with the embryo development (Fig. 6a). Conversely, *HaL1L* mRNA shows the highest value in 5 DAP embryo, gradually decreases and reaches its minimum in 30 DAP embryos (Fig. 6b). Leaf mRNA, which was found to contain both *HaL1L* and *HaWUS* mRNA, was used as reference sample (Supplemental Fig. S14).

**Fig. 6**

Steady-state levels of *HaWUS* and *HaL1L* mRNA in embryos at different DAP. Relative transcript values were calculated using leaf as reference sample. Each value is the mean ± SD of three biological replicates ($n = 3$). Values are significantly different ($^{*}P < 0.05$; $^{**}P < 0.01$) according to Tukey's test

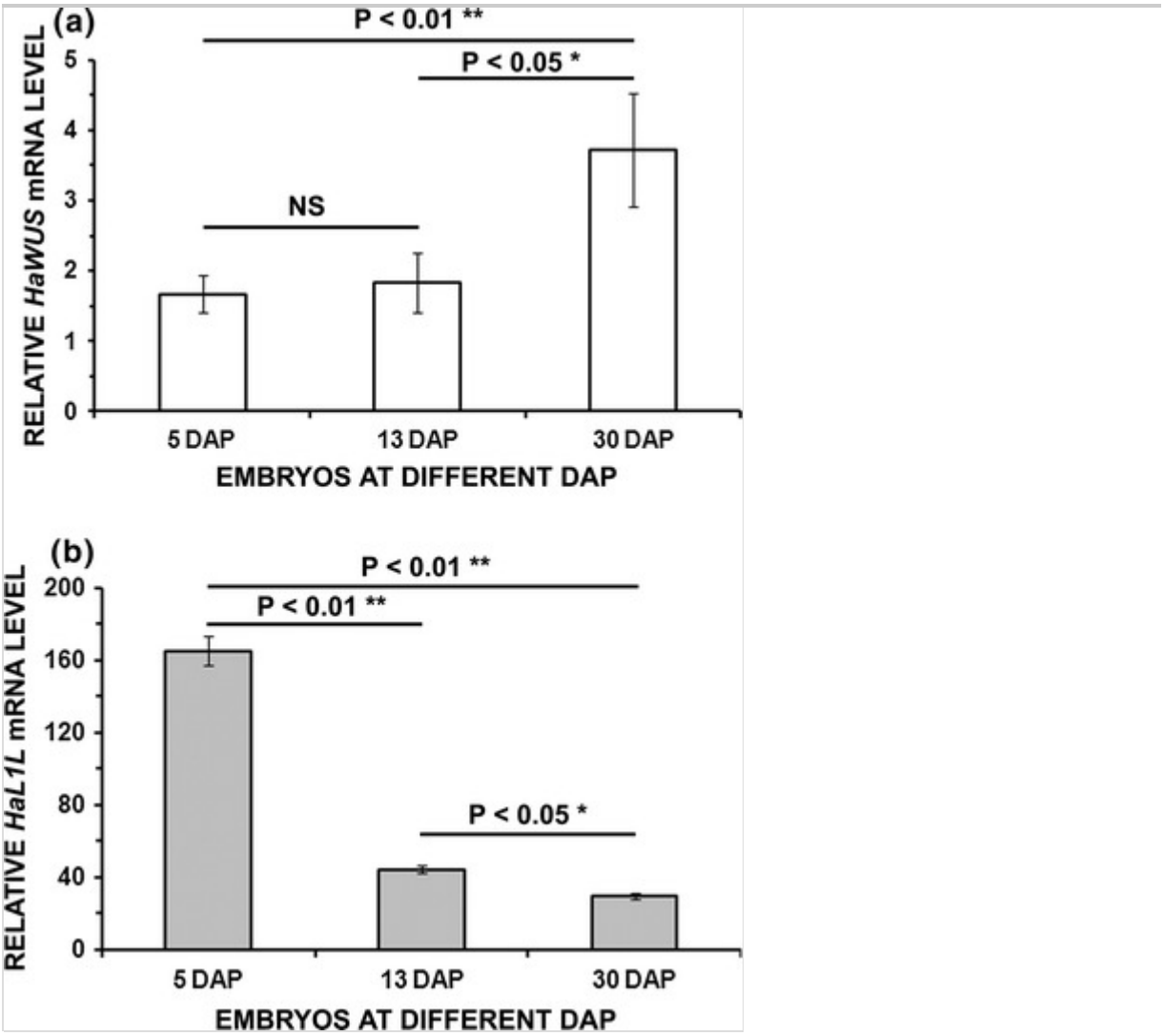


## Histone marks along *HaWUS* and *HaL1L* genomic regions revealed by ChIP analysis

A ChIP analysis was performed to detect the pattern of arrangement of the histone marks along *HaWUS* and *HaL1L* genomic regions and to examine if

changes occur during embryo development.

Our investigation has been focused on the placement of the acetylated form of histone H3 and of the histone H3 bearing a tri-methylated lysine in the fourth position of the amino acid sequence.

We have analyzed the genomic regions starting from the promoters, where we have surveyed the areas around the TATA-boxes, and a 3′END coding region (Fig. 7; Supplemental Fig. S9). Also we have analyzed a promoter region of *HaL1L* (Fig. 7; Supplemental Fig. S9), named IS1 that represents a gene section subjected to variation in the DNA methylation degree during embryo development (Salvini et al. 2012).

**Fig. 7**

Schematic representation of the *WUSCHEL* (*HaWUS*, **a**) and *LEAFY COTYLEDON1-LIKE* (*HaL1L*, **b**) genes of *Helianthus annuus*. The GenBank accession numbers for *HaWUS* and *HaL1L* are LN811433 and AJ879074, respectively. The *blue rectangles* indicate the 5′ promoter regions of both genes. The *green* and *red triangles* represent the translation start and stop codon, respectively. The *light blue rectangles* represent the exons of both genes joined by introns depicted as *lines*. For the *HaL1L*, the position of two GC rich isles (1 and 2) is reported. The primer combinations TATA-WUSF/TATA-WUSR and 3END-WUSF/3END-WUSR for *HaWUS*, and Is1-L1LF/Is1-L1LR, TATA-L1LF/TATA-L1LR, and L1L-3ENDF/L1L-3ENDR for *HaL1L* are written in *red letters* and the *arrows* indicate the 5′–3′-primer direction. The *red rectangles*, neighboring to primers, indicate the PCR-amplified products. In *brackets* is indicated the length (bp) of each PCR-amplified product

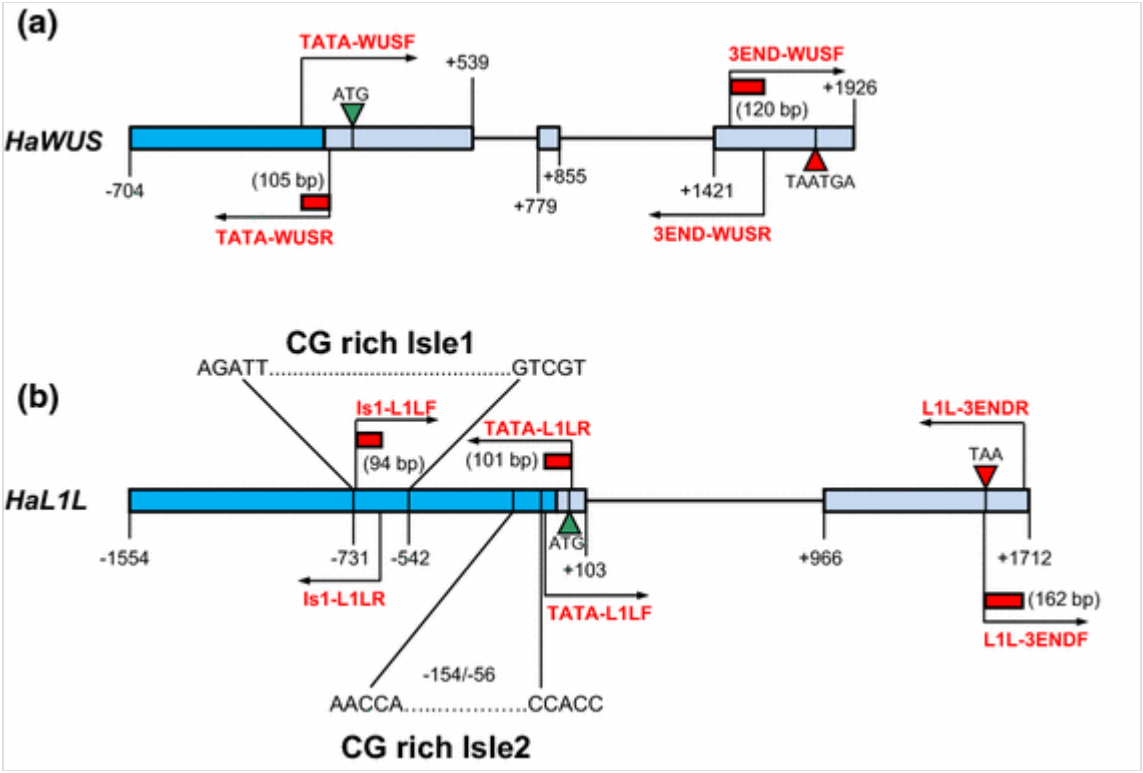


For both genes, it has been observed the same distribution of H3K4me3 showing lower levels in the regions of the TATA-boxes and higher levels in the coding parts, in addition, for *HaL1L*, the lowest amount is in the IS1 (Fig. 8a, b). Examining the embryo development, it has been revealed that H3K4me3 maintains the proportions between the different gene segments both for *HaWUS* and *HaL1L* (Supplemental Fig. S15); however, a general increase on *HaWUS*, and a decrease on *HaL1L* were revealed in 13 in comparison to 30 DAP embryos (Supplemental Fig. S15).

**Fig. 8**

Relative amounts of DNA for *HaWUS* and *HaL1L* associated with H3K4me3 as determined by ChIP-qPCR in embryos of 13 DAP (**a**) and 30 DAP (**b**). Chromatins, extracted and immunoprecipitated with anti- H3K4me3, were qPCR amplified to scan the areas around the TATA-boxes and the coding regions both for *HaWUS* and *HaL1L*. Also the IS1 promoter region of *HaL1L*, subjected to variation in the DNA methylation degree during embryo development (Salvini et al. 2012), was analyzed. Relative quantification of specific DNA levels was performed using the comparative ~~2 − Δ(ΔCt)~~$2^{-\Delta\Delta C_T}$ method (Livak and Schmittgen 2001). The obtained values were normalized to ACT2 and to INPUT DNA (chromatin before immunoprecipitation). *Bars* are means of (±SD) from three independent qPCR analyses with 3–4 different ChIP replicates for each embryo phase. All qPCR analyses were performed with three different replicates in each run for all biological samples. Values are

significantly different (*$P < 0.05$; **$P < 0.01$) according to Tukey's test

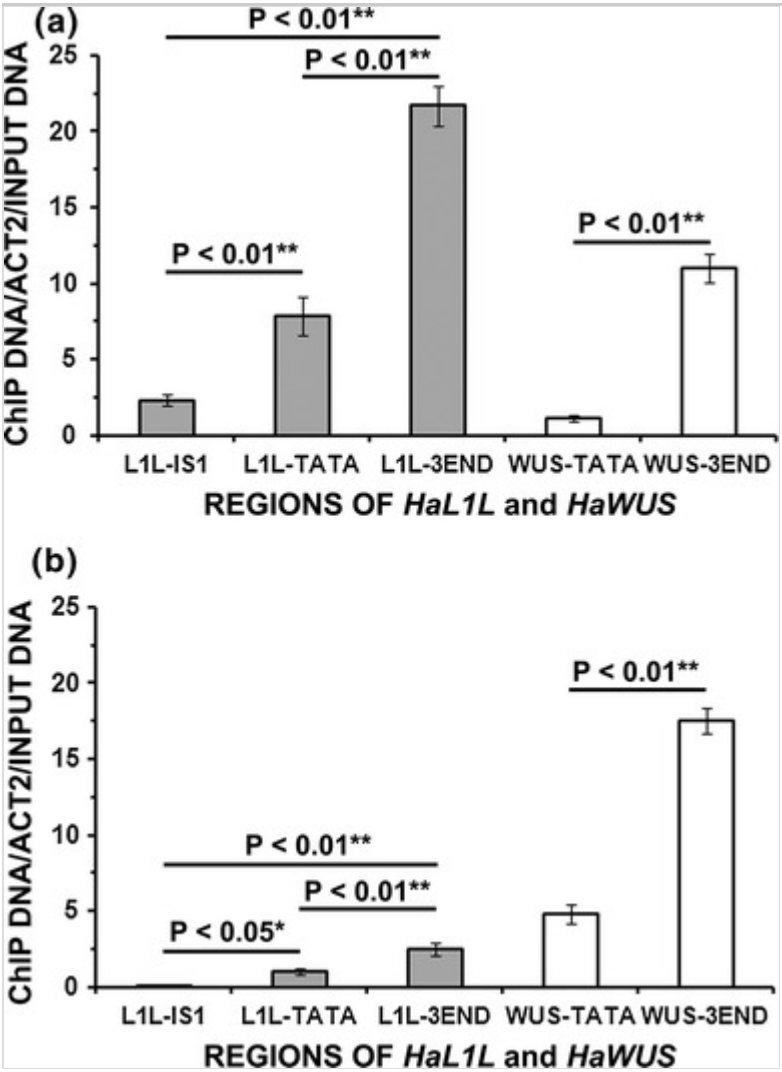


Analogous conclusions have been drawn as regards the distribution pattern along the two genes and the behavior during embryo development when the ChIP has been performed to study the linkage of acetylated H3 to both *HaWUS* and *HaL1L* (Fig. 9a, b; Supplemental Fig. S16).

**Fig. 9**

Relative amounts of DNA for *HaWUS* and *HaL1L* associated with acetylated H3 as determined by ChIP-qPCR in embryos of 13 DAP (**a**) and 30 DAP (**b**). Chromatins, extracted and immunoprecipitated with anti-acetyl H3, were qPCR amplified to scan the areas around the TATA-boxes and the coding regions both for *HaWUS* and *HaL1L*. Also the IS1 promoter region of *HaL1L*, subjected to variation in the DNA methylation degree during embryo development (Salvini et al. 2012), was analyzed. Relative quantification of specific DNA levels was performed using the comparative ~~2 − − Δ(ΔCt)~~$2^{-\Delta\Delta C_T}$ method (Livak and Schmittgen 2001).The obtained values were normalized to ACT2 and to INPUT DNA (chromatin before immunoprecipitation). *Bars* are means of (±SD) from

three independent qPCR analyses with 3–4 different ChIP replicates for each DAP embryo phase. All qPCR analyses were performed with three different replicates in each run for all biological samples. Values are significantly different (*$P < 0.05$; **$P < 0.01$) according to Tukey's test

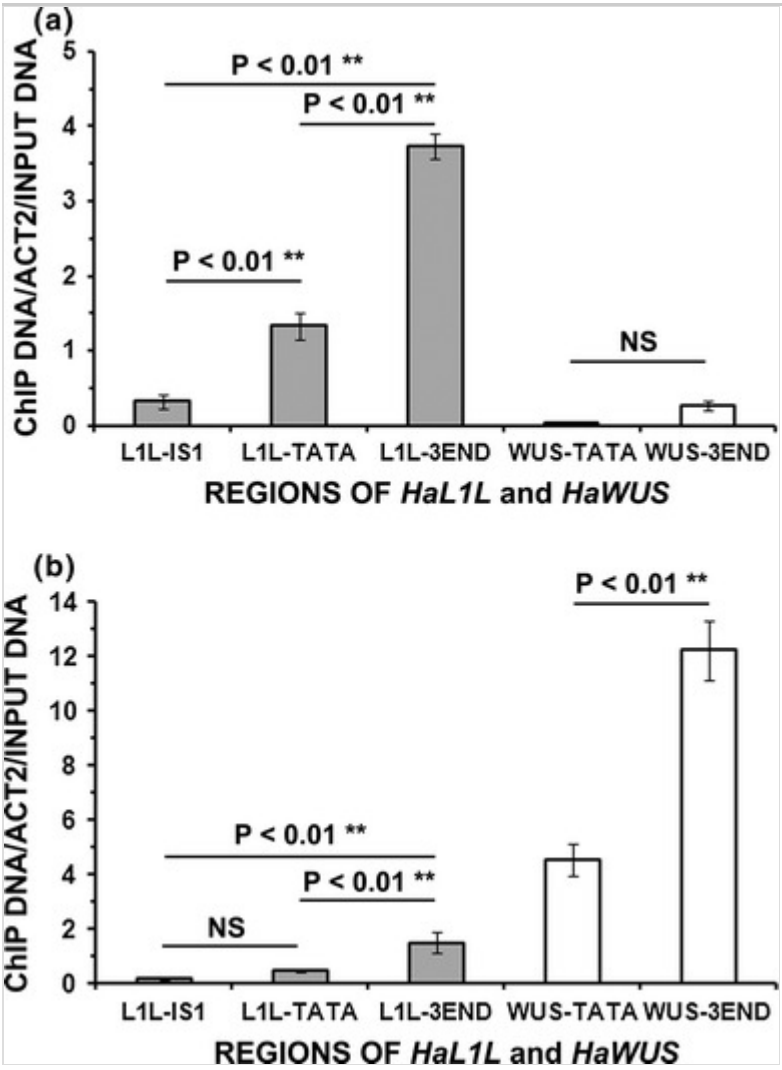


# Discussion

## WUS, a bifunctional transcription factor

Despite the positive effect on the expression of *AG* and *CLV3*, WUS must be considered a bifunctional TF (Ikeda et al. 2009). In fact, *ARABIDOPSIS RESPONSE REGULATOR7* (*ARR7*) was found to be a direct target of WUS which exerts an inhibitory effect. In *Arabidopsis*, the protein AtWUS regulates the expression of *AG* by binding the second intron and *ARR7* by binding the 5′-upstream region (Lohmann et al. 2001; Leibfried et al. 2005; Ikeda et al. 2009), in correspondence of a specific nucleotide motif named WUSATA.

Bifunctional TFs, depending on the target gene, are known both in animals (Adkins et al. 2006; Staller et al. 2015) and plants. For example, Pti4, a transcriptional activator of tomato (*Solanum lycopersicum*), and *Arabidopsis* WRKY53, activate or repress the expression of genes, depending on the nature of the promoter sequence of their target genes (Miao et al. 2004; González-Lamothe et al. 2008).

AtWUS may be functionally converted from repressor to activator by not identified factors that interact with a specific region of the protein, the "WUS box" (Kieffer et al. 2006), in the C-terminal tail. The "EAR-like" motif is also necessary for the repressive role of AtWUS, differently from the "acidic region" that has a weak positive role on gene transcription (Ikeda et al. 2009). All the above three motives are conserved in HaWUS: "acidic region" (EMFENRDQDEEQGE), "WUS box" (TLPLFPIH), and "EAR-like" (SLELSLN). HaWUS also contains the typical helix-turn-helix (HTH) of the homeodomain to make intimate contacts with the DNA of target genes (Supplemental Fig. S2).

HaWUS could have the gene *HaL1L* as a putative target. Two motives for the protein HaWUS binding have been identified in the nucleotide sequence of *HaL1L*, b subunit of a NF-Y TF, one of which is located in the intron and the other near to a 5′ region subjected to DNA methylation (Salvini et al. 2012; this report). The kind of action exerted by HaWUS on *HaL1L* has not been investigated, so we are not able to define if an activating or a repressive effect is established. However, our investigation, performed on developing embryos in sunflower, shows that the two TF mRNAs display opposite behaviors consistent with an inhibitory effect of HaWUS on *HaL1L*. This could be in agreement with the repressive action of *AtWUS* on *AtLEC1* expression during embryogenesis (Zuo et al. 2002). However, to date, no works have definitely proved whether *AtLEC1* and its closely related *AtL1L* have redundant or distinct roles, even if different function during embryogenesis seems likely considering their specific expression patterns (Kwong et al. 2003; Santos-Mendoza et al. 2008). In sunflower, the amount of *HaWUS* mRNA remains essentially the same from 5 to 13 DAP, but increases significantly with embryo development. Moreover, according to *Arabidopsis* (Mayer et al. 1998), *HaWUS* mRNA conserves the specific localization in embryo developmental stages as well as in post-embryonic tissues. On the contrary, *HaL1L* mRNA shows the highest value in 5 DAP embryos, gradually decreases and reaches its minimum in 30 DAP embryos. Bearing in mind that

AtWUS acts as both transcriptional activator and repressor, according to the target gene, e.g., *AG* and *ARR7* on which the WUSATA motives are placed in the intron and in the 5′ promoter region, respectively, it would be interesting to investigate if the position of the binding sequence makes the difference. In this instance, a change in the effect of HaWUS on *HaL1L* transcription might occur, at a restricted site or stage, depending on the WUSATA motif bound. **AQ3**

## A complex regulation for *HaWUS* is shown by the in silico analysis

The in silico prediction of potential regulatory sites and of their organization allows to greatly improve our understanding of gene expression and regulation, and limits the amount of protein-DNA interactions to be tested experimentally (Franco-Zorrilla et al. 2014; Keilwagen and Grau 2015). Therefore, an increasing number of software packages are developed and made available on the network [e.g., comprehensive lists are: (1) Plant Promoter and Regulatory Element Resources at the Arabidopsis Information Resource (TAIR) Tair: https://www.arabidopsis.org/portals/genAnnotation /genome_annotation_tools/cis_element.jsp; (2) gene expression regulatory sites and TFs—at the Health Sciences Library System (University of Pittsburgh, USA): http://www.hsls.pitt.edu /obrc/index.php?page=promoter_transcription_factors]. However, not all motifs are functional elements or are simultaneously active, since TFs action is dependent on the context. Therefore, only rigorous testing can determine the actual working significance of each predicted specific target site (Geertz and Maerkl 2010; Salvini et al. 2012).

In *HaWUS*, a number of motifs, scattered throughout the nucleotide sequence, are indicative of complex relationship including those of WUS with its gene itself and with NF-Ys, to which *HaL1L* belongs. Interesting new connections are suggested that lead back to the involvement in regulatory mechanisms sensitive to light or related to the circadian clock regulation and hormones, such as gibberellins (GAs), abscisic acid (ABA), and auxin (Su et al. 2009; Busch et al. 2010). Putative links are also identified for genes that were already found to act on *WUS*, such as *BELLRINGER* (Bao et al. 2004); hormone-related *APETALA2* (Liu et al. 2014), *ASYMMETRIC LEAVES1* (*AS1*)–*AS2* complex (Lodha et al. 2013), and *POLYCOMB* group genes (*PcG*) (Liu et al. 2011).

In the context of the present report, a particular interest concerns the

identification of putative motifs that lead back to the idea that post-translational of histones, mainly methylation and acetylation, can participate to *HaWUS* gene regulation.

MatInspector software recognizes a G/A-rich region of *HaWUS* nucleotide sequence that represents the putative site for the binding of Basic Pentacysteine Proteins (BPCs). BPCs are retained functionally equivalent (Berger and Dubreucq 2012; Simonini et al. 2012) to GAGA-factors (GAFs) that are not yet recognized in plants on the basis of conserved amino acid sequences. In animals, e.g., *Drosophila melanogaster*, GAGA-factors can interact with GAGAG sequences to recruit TrxG and PcG (Berger and Dubreucq 2012). The general mechanisms of PcG protein functions are well preserved although, in plants, different players appeared during evolution (Hennig and Derkacheva 2009). PcG and Trithorax (TrxG) complexes control the expression of developmental regulator genes through modifications of the chromatin status, e.g., the deposition of the repressive H3K27me3 and the activator H3K4me3, respectively (Aichinger et al. 2009; Berr et al. 2011; Deng et al. 2013; Derkacheva and Hennig 2014; Mozgova and Hennig 2015).

The involvement of histone H3 methylation in *HaWUS* regulation is also suggested by the presence of several other putative binding motives; e.g., PROMO software finds DNA-binding sequences for the ALFIN1-like protein implied into the switch from the H3K4me3-associated active to the H3K27me3-associated repressive transcription state of seed developmental genes promoting seed germination (Molitor et al. 2014).

Other putative DNA sites for the binding of TFs resulted in additional interest, because it can represent members of a most vast network to which different post-translational histone modifications, methylation, and acetylation may participate. They are YY1, the MYB-type transcription AS1/AS2 complex, and AG. YY1, a multifunctional TF, acts as transcriptional activator and/or repressor through the deposition of histone modifications (H3 acetylation/deacetylation and H3K27 methylation) (Srinivasan and Atchison 2004; Wilkinson et al. 2006; He et al. 2013; Atchison 2014; Lai et al. 2014). Analogously, AS1/AS2 complex and AG were somehow correlated among themselves and both with H3K27 methylation (Deng et al. 2013, Lodha et al. 2013) and histone acetylation (Srinivasan and Atchison 2004; Luo et al. 2012; Lodha et al. 2013).

The acetylation is another modification associated to gene regulation that in *A. thaliana* affects K residues of the histones H3 and H4 (Berr and Shen 2010; Berr et al. 2011). Specific acetylases (HATs) and deacetylases (HDCs) act antagonistically to maintain the homeostatic balance of the histone acetylation. Also HDC1 enhancer was identified that strengthen the repressive effect of histone deacetylation on transcription (Perrella et al. 2013).

In *A. thaliana*, a histone acetylase, which is coded by *AtGCN5* and is involved in both long-term and short-term dynamic transcriptional regulations (Benhamed et al. 2008; Berr et al. 2011), limits the domain of *WUS* expression within the floral meristem turning on a *WUS* repressor through the *WUS/AG* pathway (Bertrand et al. 2003). Moreover, in the termination of floral stem cell maintenance in *A. thaliana*, AG represses *WUS* expression recruiting PcG proteins to deposit H3K27me3 (Liu et al. 2011) with a still unknown way.

A final remark concerns a particular regulatory region that might be involved in the control of tissue specificity and levels of *HaWUS* transcription. In sunflower, a 56 bp region is identified, from −515 to −570 bp upstream the TSS (Supplementary Fig. S1), that could be equivalent to a 57 bp control region necessary for transcription of *AtWUS* in niches of the inflorescence meristem (Bäurle and Laux 2005).

## Acetylated H3 and tri-methylated H3K4 coupled to *HaWUS* and *HaL1L* during embryo development

Based on the above, we decided to perform a parallel analysis of histone patterns associated with both *HaWUS* and *HaL1L* during embryo development, referring to the acetylated histone H3 and to K4m3 of the same histone, two chromatin marks positively regulating gene transcription. Our interest in *HaL1L* derives from its presumed relationship with *HaWUS* (Salvini et al. 2012; this report).

The same distribution patterns of H3K4me3 linked to short genes, as described for *A. thaliana* seedlings (Zhang et al. 2009), were observed for both *HaWUS* and *HaL1L* in 5 and 30 DAP embryos, respectively, (i.e., a lower concentration of the histone mark in the promoter region in the respect to the coding frame). In fact, Zhang et al. (2009) pointed out that as gene length decreases, significantly more genes were found to contain H3K4me3 in their 3′ region. In particular, in the last, 200 bp short genes contain higher level of

HeK4me3 than long genes. This is the case of the analyzed *HaWUS* region located around 190 bp from the translation stop codons.

Similar observations are also reported in a study about H3K4me2, H3K4me3, H3K9ac, and H3K27ac in *O. sativa.* Histone modifications were found significantly enriched around transcription start sites (TSSs) but seldom near transcription terminal sites (TTSs) of genes, which are not transposable elements. Interestingly, the summits of the analyzed four histone modification peaks were in the gene body region, downstream of the TSSs (Du et al. 2013).

Finally, as regards *HaL1L*, the lowest amounts of both acetylated H3 and H3K4me3 were individuated coupled with the IS1 promoter region, suggesting a negative correlation with DNA methylation. This latter observation is in agreement with what detected in *A. thaliana* seedlings where, however, the loss of DNA methylation generally does not triggers hyper-H3K4me (Zhang et al. 2009).

Our information on the general progressive decrease in H3K4me3 and acetylated H3 linked to *HaL1L*, in contrast to the enrichment of *HaWUS* genomic region in both positive histone marks, during the transition from 13 to 30 DAP, are in agreement with our study on mRNA steady states. In fact, the transcription of *HaL1L* decreases meanwhile the transcription of *HaWUS* increases.

The demonstrated in vitro link of HaWUS/*HaL1L* supports the hypothesis of a direct interaction of the WUS protein with the *HaL1L* gene during zygotic embryo development, and the hypothesis of an inhibitory effect is corroborated by the opposite transcriptional behavior. However, at 13 DAP, the strong decrease in *HaL1L* transcript is uncoupled with a prominent increase of *HaWUS* transcript. It is likely that, during embryo maturation, *HaL1L* transcription is controlled by a complex gene network where *HaWUS* is one of the key players. In the absence of direct experimental evidence, it is difficult to draw any definitive conclusions, so at the moment we are only able to present the data. However, it may be interesting to note that in a developmental path of somatic embryogenesis redefined by *WUS* overexpression, *LEC1* is repressed. This suggests a predominance of *WUS* on *LEC1*, whose driving force for embryo cell differentiation must be excluded in order to fully maintain the embryonic potential (Zuo et al. 2002). In turn, HaL1L could regulate *HaWUS* by the binding to motifs for NF-Y present on

*HaWUS* genomic nucleotide sequence. Moreover, the sharing, between *HaWUS* and *HaL1L*, of binding motives for several TFs, e.g., *LFY* or *BELLRINGER*, could indicate the sharing of some complicate gene network.

The meaning of *WUS* expression in 30 DAP embryos remains to be explained. It must be kept in mind that *WUS* may have unexpected roles. In *Vitis vinifera*, Gambino et al. (2011) demonstrated that the level of *VvWUS* expression was higher in embryos at the cotyledonary stage with respect to the torpedo stage. Furthermore, time-dependent control of *WOX* genes expression has been observed in *Zea mays* (Nardmann et al. 2007), *Araucaria angustifolia* (Schlög et al. 2012), and *Picea abies* (Palovaara et al. 2010; Zhu et al. 2014) during zygotic and somatic embryogenesis.

*Author contribution statement* MS designed the experiments and analyses. MS, MF, LG, and CP performed data collection and data processing. MS wrote the manuscript, and all authors were involved in results presentation, discussion, and preparation of the final manuscripts.

## Electronic supplementary material

Below is the link to the electronic supplementary material.

Supplementary material 1 (PDF 157 kb)

Supplementary material 2 (PDF 52 kb)

Supplementary material 3 (PDF 132 kb)

Supplementary material 4 (PDF 142 kb)

Supplementary material 5 (PDF 100 kb)

Supplementary material 6 (PDF 128 kb)

Supplementary material 7 (PDF 2978 kb)

Supplementary material 8 (PDF 136 kb)

Supplementary material 9 (PDF 69 kb)

Supplementary material 10 (PDF 142 kb)

Supplementary material 11 (PDF 31 kb)

Supplementary material 12 (PDF 91 kb)

Supplementary material 13 (PDF 138 kb)

Supplementary material 14 (PDF 99 kb)

Supplementary material 15 (PDF 152 kb)

Supplementary material 16 (PDF 76 kb)

Supplementary material 17 (PDF 176 kb)

Supplementary material 18 (PDF 37 kb)

# References

Adkins NL, Hagerman TA, Georgel P (2006) GAGA protein: a multi-faceted transcription factor. Biochem Cell Biol 84:559–567

Aichinger E, Villar CBR, Farrona S, Reyes JC, Henning L, Köhler C (2009) CHAD3 proteins and polycomb group proteins antagonistically determine cell identity in Arabidopsis. PLoS Genet 5(8):e1000605

Altschul SF, Madden TL, Schäffer AA, Zhang J, Zhang Z, Miller W, Lipman DJ (1997) Gapped BLAST and PSI-BLAST: a new generation of protein database search programs. Nucleic Acids Res 25:3389–3402

Atchison ML (2014) Function of YY1 in long-distance DNA interactions. Front Immunol 5:45

Bao X, Franks RG, Levin JZ, Liu Z (2004) Repression of *AGAMOUS* by *BELLRINGER* in floral and inflorescence meristems. Plant Cell 16:1478–1489

Bateman A, Birney E, Cerruti L, Durbin R, Etwiller L, Eddy SR, Griffiths-Jones S, Howe KL, Marshall M, Sonnhammer ELL (2002) The pfam protein families database. Nucleic Acids Res 30:276–280

Bäurle I, Laux T (2005) Regulation of *WUSCHEL* transcription in the stem cell niche of the Arabidopsis shoot meristem. Plant Cell 17:2271–2280

Benhamed M, Martin-Magniette M-L, Taconnat L, Bitton F, Servet C, De Clercq R, De Meyer B, Buysschaert C, Rombauts S, Villarroel R, Aubourg S, Beynon J, Bhalerao RP, Coupland G, Gruissem W, Menke FLH, Weisshaar B, Renou J-P, Zhou D-X, Hilson P (2008) Genome-scale Arabidopsis promoter array identifies targets of the histone acetyltransferase GCN5. Plant J 56:493–504

Berger N, Dubreucq B (2012) Evolution goes GAGA: GAGA binding proteins across kingdoms. Biochim Biophys Acta 1819:863–868

Berr A, Shen WH (2010) Molecular mechanisms in epigenetic regulation of plant growth and development. Plant Dev Biol Biotech Perspect 2:325–344

**AQ4**

Berr A, Shafiq S, Shen WH (2011) Histone modifications in transcriptional activation during plant development. Biochim Biophys Acta 1809:567–576

Berti F, Fambrini M, Turi M, Bertini D, Pugliesi C (2005) Mutations of corolla symmetry affect carpel and stamen development in *Helianthus annuus*. Can J Bot 83:1065–1072

Bertrand C, Bergounioux C, Domenichini S, Delarue M, Zhou D-X (2003) Arabidopsis histone acetyltransferase AtGCN5 regulates the floral meristem activity through the *WUSCHEL/AGAMOUS* pathway. J Biol Chem 278:28246–28251

Brand U, Fletcher JC, Hobe M, Meyerowitz EM, Simon R (2000) Dependence of stem cell fate in *Arabidopsis* on a feedback loop regulated by *CLV3* activity. Science 289:617–619

Braybrook SA, Harada JJ (2008) LECs go crazy in embryo development. Trends Plant Sci 13:624–630

Busch W, Miotk A, Ariel FD, Zhao Z, Forner J, Daum G, Suzaki T, Schuster C, Schultheiss SJ, Leibfried A, Haubeiss S, Ha N, Chan RL, Lohmann JU (2010) Transcriptional control of a plant stem cell niche. Dev Cell 18:849–861

Cartharius K, Frech K, Grote K, Klocke B, Haltmeier M, Klingenhoff A, Frisch M, Bayerlein M, Werner T (2005) MatInspector and beyond: promoter analysis based on transcription factor binding sites. Bioinformatics 21:2933–2942

~~Chenlong L, Keqiang W, Guohua F, Yin L, Yujuan Z, Xiaodong L, Yi Z, Lining T, Shangzhi H (2009) Regulation of oleosin expression in developing peanut (*Arachis hypogaea* L.) embryos through nucleosome loss and histone modifications. J Exp Bot 60:4371–4382~~

Chiappetta A, Fambrini M, Petrarulo M, Rapparini F, Michelotti V, Bruno L, Greco M, Baraldi R, Salvini M, Pugliesi C, Bitonti MB (2009) Ectopic expression of *LEAFY COTYLEDON-LIKE* gene and localized auxin accumulation mark embryogenic competence in epiphyllous plants of *Helianthus annuus* × *H. tuberosus*. Ann Bot 103:735–747

Collings CK, Waddell PJ, Anderson JN (2013) Effects of DNA methylation on nucleosome stability. Nucleic Acids Res 41:2918–2931

Combet C, Jambon M, Deléage G, Geourjon C (2002) Geno3D: automatic comparative molecular modelling of protein. Bioinformatics 18:213–214

De Smet I, Lau S, Mayer U, Jürgens G (2010) Embryogenesis—the humble

beginnings of plant life. Plant J 61:959–970

Deng W, Buzas DM, Ying H, Robertson M, Taylor J, Peacock WJ, Dennis ES, Helliwell C (2013) Arabidopsis Polycomb Repressive Complex 2 binding sites contain putative GAGA factor binding motifs within coding regions of genes. BMC Genom 14:593

Derkacheva M, Hennig L (2014) Variations on a theme: polycomb group proteins in plants. J Exp Bot 65:2769–2784

Doerner P (2001) Plant meristems: a ménage à trois to end it all. Curr Biol 11:R785–R787

Du Z, Li H, Wei Q, Zhao X, Wang C, Zhu Q, Yi X, Xu W, Liu XS, Jin W, Su Z (2013) Genome-wide analysis of histone modifications: H3K4me2, H3K4me3, H3K9ac, and H3K27ac in *Oryza sativa* L. Japonica. Mol Plant 6:1463–1472

Falquet L, Pagni M, Bucher P, Hulo N, Sigrist CJ, Hofmann K, Bairoch A (2002) The PROSITE database, its status in 2002. Nucleic Acids Res 30:235–238

Fambrini M, Durante C, Cionini G, Geri C, Giorgetti L, Michelotti V, Salvini M, Pugliesi C (2006) Characterization of *LEAFY COTYLEDON1-LIKE* gene in *Helianthus annuus* and its relationship with zygotic and somatic embryogenesis. Dev Genes Evol 216:253–264

Fambrini M, Salvini M, Pugliesi C (2011) A transposon-mediate inactivation of a *CYCLOIDEA*-like gene originates polysymmetric and androgynous ray flowers in *Helianthus annuus*. Genetica 139:1521–1529

Farré D, Roset R, Huerta M, Adsuara JE, ~~Llorenç~~ Roselló L, ~~Mar~~ Albà MM, Messeguer X (2003) Identification of patterns in biological sequences at the ALGGEN server: PROMO and MALGEN. Nucleic Acids Res 31:3651–3653

Finley A, Copeland RA (2014) Small molecule control of chromatin remodeling. Chem Biol 18:1196–1210

Franco-Zorrilla JM, López-Vidriero I, Carrasco JL, Godoy M, Vera P,

Solano R (2014) DNA-binding specificities of plant transcription factors and their potential to define target genes. Proc Natl Acad Sci USA 111:2367–2372

Furutani M, Vernoux T, Traas J, Kato T, Tasaka M, Aida M (2004) *PIN-FORMED1* and *PINOID* regulate boundary formation and cotyledon development in *Arabidopsis* embryogenesis. Development 131:5021–5030

Gambino G, Minuto M, Boccacci P, Perrone I, Vallania R, Gribaudo I (2011) Characterization of expression dynamics of WOX homeodomain transcription factors during somatic embryogenesis in *Vitis vinifera*. J Exp Bot 62:1089–1101

Geertz M, Maerkl SJ (2010) Experimental strategies for studying transcription factor-DNA binding specificities. Brief Funct Genomics 5–6:362–373

~~Goldberg AD, Allis CD, Bernstein E (2007) Epigenetics: a landscape takes shape. Cell 23:635–638~~

González-Lamothe R, Boyle P, Dulude A, Roy V, Lezin-Doumbou C, Kaur GS, Bouarab K, Despres C, Brisson N (2008) The transcriptional activator pti4 is required for the recruitment of a repressosome nucleated by repressor SEBF at the potato *PR-10a* gene. Plant Cell 20:3136–3147

Gordon SP, Chickarmane VS, Ohno C, Meyerowitz EM (2009) Multiple feedback loops through cytokinin signaling control stem cell number within the *Arabidopsis* shoot meristem. Proc Natl Acad Sci USA 106:16529–16534

Guex N, Peitsch MC (1997) SWISS-MODEL and the Swiss-PdbViewer: an environment for comparative protein modeling. Electrophoresis 18:2714–2723

Haecker A, Groß-Hardt R, Geiges B, Sarkar A, Breuninger H, Herrman M, Laux T (2004) Expression dynamics of *WOX* genes mark cell fate decisions during early embryonic patterning in *Arabidopsis thaliana*. Development 131:657–668

Hay A, Barkoulas M, Tsiantis M (2004) PINning down the connections:

transcription factors and hormones in leaf morphogenesis. Curr Opin Plant Biol 7:575–581

Hay A, Barkoulas M, Tsiantis M (2006) ASYMMETRIC LEAVES1 and auxin activities converge to repress *BREVIPEDICELLUS* expression and promote leaf development in *Arabidopsis*. Development 133:3955–3961

He C, Huang H, Xu L (2013) Mechanisms guiding Polycomb activities during gene silencing in *Arabidopsis thaliana*. Front Plant Sci 4:454

Hennig L, Derkacheva M (2009) Diversity of Polycomb group complexes in plants: same rules, different players? Trends Genet 25:414–423

Hewezi T, Petitprez M, Gentzbittel L (2006) Primary metabolic pathways and signal transduction in sunflower (*Helianthus annuus* L.): comparison of transcriptional profiling in leaves and immature embryos using cDNA microarrays. Planta 223:948–964

Hilioti Z, Ganopoulos I, Bossis I, Tsaftaris A (2014) LEC1-LIKE paralog transcription factor: how to survive extinction and fit in NF-Y protein complex. Gene 543:220–233

Ikeda M, Mitsuda N, Ohme-Takagi M (2009) *Arabidopsis* WUSCHEL is a bifunctional transcription factor that acts as a repressor in stem cell regulation and as an activator in floral patterning. Plant Cell 21:3493–3505

Iwasaki M, Paszkowski J (2014) Epigenetic memory in plants. EMBO J 33:1987–1998

Jackson D (1991) In situ hybridisation in plants. In: Bowles DJ, Gurr GJ, McPherson M (eds) Molecular plant pathology: a practical approach. Oxford University Press, Oxford, pp 163–174

Keilwagen J, Grau J (2015) Varying levels of complexity in transcription factor binding motifs. Nucleic Acids Res. doi:10.1093/nar/gkv577

Kieffer M, Stern Y, Cook H, Clerici E, Maulbetsch C, Laux T, Davies B (2006) Analysis of the transcription factor WUSCHEL and its functional homologue in *Antirrhinum* reveals a potential mechanism for their roles in meristem maintenance. Plant Cell 18:560–573

Kim DH, Su S (2014) Polycomb-mediated gene silencing in *Arabidopsis thaliana*. Mol Cells 37:841–850

Kwon CS, Chen C, Wagner D (2005) *WUSCHEL* is a primary target for transcriptional regulation by SPLAYED in dynamic control of stem cell fate in *Arabidopsis*. Genes Dev 19:992–1003

Kwong RW, Bui AQ, Lee H, Kwong LW, Fischer RL, Goldberg RB, Harada JJ (2003) LEAFY COTYLEDON1-LIKE defines a class of regulators essential for embryo development. Plant Cell 15:5–18

Lai Z, Schluttenhofer CM, Bhide K, Shreve J, Thimmapuram J, Lee SY, Yun D-J, Mengiste T (2014) MED18 interaction with distinct transcription factors regulates multiple plant functions. Nat Commun 5:3064

Laux T, Mayer KF, Berger J, Jürgens G (1996) The *WUSCHEL* gene is required for shoot and floral meristem integrity in *Arabidopsis*. Development 122:87–96

Lawrence RJ, Earley K, Pontes O, Silva M, Chen ZJ, Neves N, Viegas W, Pikaard CS (2004) A concerted DNA methylation/histone methylation switch regulates rRNA gene dosage control and nucleolar dominance. Mol Cell 13:599–609

Leibfried A, To JP, Busch W, Stehling S, Kehle A, Demar M, Kieber JJ, Lohmann JU (2005) WUSCHEL controls meristem function by direct regulation of cytokinin-inducible response regulators. Nature 438:1172–1175

Lenhard M, Bohnert A, Jürgens G, Laux T (2001) Termination of stem cell maintenance in *Arabidopsis* floral meristems by interactions between *WUSCHEL* and *AGAMOUS*. Cell 105:805–814

Li C, Wu K, Fu G, Li Y, Zhong Y, Lin X, Zhou Y, Tian L, Huang S (2009) Regulation of oleosin expression in developing peanut (*Arachis hypogaea* L.) embryos through nucleosome loss and histone modifications. J Exp Bot 60:4371–4382

Lian G, Ding Z, Wang Q, Zhang D, Xu J (2014) Origins and evolution of WUSCHEL-related homeobox protein family in plant kingdom. Sci World

J. 2014:534140 doi:10.1155/2014/534140

Liu X, Kim YJ, Müller R, Yumul RE, Liu C, Pan Y, Cao X, Goodrich J, Chen X (2011) *AGAMOUS* terminates floral stem cell maintenance in *Arabidopsis* by directly repressing *WUSCHEL* through recruitment of Polycomb Group proteins. Plant Cell 23:3654–3670

Liu X, Dinh TT, Li D, Shi B, Li Y, Cao X, Guo L, Pan Y, Jiao Y, Chen X (2014) *AUXIN RESPONSE FACTOR 3* integrates the functions of *AGAMOUS* and *APETALA2* in floral meristem determinacy. Plant J 80:629–641

Livak KJ, Schmittgen TD (2001) Analysis of relative gene expression data using Real-Time quantitative PCR and the $2^{-\Delta\Delta C_T}$ method. Methods 25:402–408

Lodha M, Marco CF, Timmermans MCP (2013) The ASYMMETRIC LEAVES complex maintains repression of KNOX homeobox genes via direct recruitment of Polycomb-repressive complex2. Genes Dev 27:596–601

Lohmann JU, Hong RL, Hobe M, Busch MA, Parcy F, Simon R, Weigel D (2001) A molecular link between stem cell regulation and floral patterning in *Arabidopsis*. Cell 105:793–803

Lotan T, Ohto M, Yee KM, West MAL, Lo R, Kwong RW, Yamagishi K, Fischer RL, Goldberg RB, Harada JJ (1998) *Arabidopsis* LEAFY COTYLEDON1 is sufficient to induce embryo development in vegetative cells. Cell 93:1195–1205

Luo M, Yu CW, Chen FF, Zhao L, Tian G, Liu X, Cui Y, Yang JY, Wu K (2012) Histone deacetylase HDA6 is functionally associated with AS1 in repression of *KNOX* genes in *Arabidopsis*. PLoS Genet 8(12):e1003114

Manzano C, Ramirez-Parra E, Casimiro I, Otero S, Desvoyes B, De Rybel B, Beeckman T, Casero P, Gutierrez C, del Pozo C (2012) Auxin and epigenetic regulation of *SKP2B*, an F-box that represses lateral root formation. Plant Physiol 160:749–762

Mayer KFX, Schoof H, Haecker A, Lenhard M, Jürgens G, Laux T (1998)

Role of *WUSCHEL* in regulating stem cell fate in the *Arabidopsis* shoot meristem. Cell 95:805–815

Messeguer X, Escudero R, Farré D, Nuñez O, Martínez J, ~~Mar~~ Albà MM (2002) PROMO: detection of known transcription regulatory elements using species-tailored searches. Bioinformatics 18:333–334

Miao Y, Laun T, Zimmermann P, Zentgraf U (2004) Targets of the WRKY53 transcription factor and its role during leaf senescence in *Arabidopsis*. Plant Mol Biol 55:853–867

Molitor AM, Bu Z, Yu Y, Shen WH (2014) *Arabidopsis* AL PHD-PRC1 complexes promote seed germination through H3K4me3-to-H3K27me3 chromatin state switch in repression of seed developmental genes. PLoS Genet 10(1):e1004091

Mozgova I, Hennig L (2015) The Polycomb group protein regulatory network. Annu Rev Plant Biol 66:269–296

Nardmann J, Zimmermann R, Durantini D, Krantz E, Werr W (2007) *WOX* gene phylogeny in *Poaceae*: a comparative approach addressing leaf and embryo development. Mol Biol Evol 24:2474–2484

~~Ng DW, Wang T, Chandrasekharan MB, Aramayo R, Kertbundit S, Hall TC (2007) Plant SET domain-containing proteins: structure, function and regulation. Biochim Biophys Acta 1769:316–329~~

Palovaara J, Hallberg H, Stasolla C, Hakman I (2010) Comparative expression pattern analysis of *WUSCHEL-~~RELATED~~ ~~HOMEOBOX~~related homeobox 2* (*WOX2*) and *WOX8/9* in developing seeds and somatic embryos of the gymnosperm *Picea abies*. New Phytol 188:122–135

Perrella G, Lopez-Vernaza MA, Carr C, Sani E, Gosselé V, Verduyn C, Kellermeier F, Hannah MA, Amtmann A (2013) Histone Deacetylase Complex1 expression level titrates plant growth and abscisic acid sensitivity in *Arabidopsis*. Plant Cell 25:3491–3505

Ptashne M (2013a) Faddish stuff: epigenetics and the inheritance of acquired characteristics. FASEB J 27:1–2

Ptashne M (2013b) Epigenetics: core misconcept. Proc Natl Acad Sci USA 110:7101–7103

Rivera C, Gurard-Levin ZA, Almouzni G, Loyola A (2014) Histone lysine methylation and chromatin replication. Biochim Biophys Acta 1839:1433–1439

Rosinski JA, Atchley WR (1999) Molecular evolution of helix-turn-helix proteins. J Mol Evol 49:301–309

Salvini M, Sani E, Fambrini M, Pistelli L, Pucciariello C, Pugliesi C (2012) Molecular analysis of a sunflower gene encoding an homologous of the B subunit of a CAAT binding factor. Mol Biol Rep 39:6449–6465

Santos-Mendoza M, Dubreucq B, Baud S, Parcy F, Caboche M, Lepiniec L (2008) Deciphering gene regulatory networks that control seed development and maturation in Arabidopsis. Plant J 54:608–620

Sarkar AK, Luijten M, Miyashima S, Lenhard M, Hashimoto T, Nakajima K, Scheres B, Heidstra R, Laux T (2007) Conserved factors regulate signalling in *Arabidopsis thaliana* shoot and root stem cell organizers. Nature 446:811–814

Scheres B (2007) Stem-cell niches: nursery rhymes across kingdoms. Nat Rev Mol Cell Biol 8:345–354

Schlög PS, ~~Wendt~~ dos Santos ALW, Viera LdoN, Floh EIS, Guerra MP (2012) Cloning and expression of embryogenesis-regulating genes in *Araucaria angustifolia* (Bert.) O. Kuntze (Brazilian Pine). Genet Mol Biol 35:172–181

Schoof H, Lenhard M, Haecker A, Mayer KF, Jürgens G, Laux T (2000) The stem cell population of *Arabidopsis* shoot meristems in maintained by a regulatory loop between the *CLAVATA* and *WUSCHEL* genes. Cell 100:635–644

Shiraishi H, Okada K, Shimura Y (1993) Nucleotide sequences recognized by the AGAMOUS MADS domain of *Arabidopsis thaliana* in vitro. Plant J 4:385–398

Siebert PD, Chenchik A, Kellog DE, Lukyanov KA, Lukyanov SA (1995) An improved method for walking in uncloned genomic DNA. Nucleic Acids Res 23:1087–1088

Simonini S, Roig-Villanova I, Gregis V, Colombo B, Colombo L, Kater MM (2012) BASIC PENTACYSTEINE proteins mediate MADS domain complex binding to the DNA for tissue-specific expression of target genes in *Arabidopsis*. Plant Cell 24:4163–4172

Sneath PHA, Sokal R (1973) Numerical taxonomy. WH Freeman and Company, San Francisco, pp 230–234

Sreenivasulu N, Wobus U (2013) Seed-development programs: a systems biology-based comparison between dicots and monocots. Annu Rev Plant Biol 64:189–217

Srinivasan L, Atchison ML (2004) YY1 DNA binding and PcG recruitment requires CtBP. Genes Dev 18:2596–2601

Staller MV, Vincent BJ, Bragdon MDJ, Lydiard-Martin T, Wunderlich Z, Estrada J, DePace AH (2015) Shadow enhancers enable Hunchback bifunctionality in the *Drosophila* embryo. Proc Natl Acad Sci USA 112:785–790

Steffen PA, Ringrose L (2014) What are memories made of? How polycomb and trithorax proteins mediate epigenetic memory. Nat Rev Mol Cell Biol 15:340–356

Stone SL, Kwong LW, Yee KM, Pelletier J, Lepiniec L, Fischer RL, Goldberg RB, Harada JJ (2001) *LEAFY COTYLEDON2* encodes a B3 domain transcription factor that induces embryo development. Proc Natl Acad Sci USA 98:11806–11811

Su Y, Zhao XY, Liu YB, Zhang C, O'Neill SD, Zhang XS (2009) Auxin-induced *WUS* expression is essential for embryonic stem cell renewal during somatic embryogenesis in Arabidopsis. Plant J 59:448–460

Sun B, Looi L-S, Guo S, He Z, Gan E-S, Huang J, Xu Y, Wee W-Y, Ito T (2014) Timing mechanism dependent on cell division is invoked by Polycomb eviction in plant stem cells. Science 343:6170.

doi:10.1126/science.1248559

Tamura K, Dudley J, Nei M, Kumar S (2007) MEGA4: molecular evolutionary genetics analysis (MEGA) software version 4.0. Mol Biol Evol 24:1596–1599

Tten Hove CA, Lu K-J, Weijers D (2015) Building a plant: cell fate specification in the early *Arabidopsis* embryo. Development 142:420–430

van der Graaff E, Laux T, Rensing SA (2009) The WUS homeobox-containing (WOX) protein family. Genome Biol 10:248

Wilkinson FH, Park K, Atchison ML (2006) Polycomb recruitment to DNA *in vivo* by the YY1 REPO domain. Proc Natl Acad Sci USA 103:19296–19301

Wingender E, Chen X, Fricke E, Geffers R, Hehl R, Liebich I, Krull M, Matys V, Ohnhäuser R, Prüß M, Schacherer F, Thiele S, Urbach S (2001) The TRANSFAC system on gene expression regulation. Nucleic Acids Res 29:281–283

Wu SC, Zhang Y (2010) Active DNA demethylation: many roads lead to Rome. Nat Rev Mol Cell Biol 11:607–620

Yadav RK, Perales M, Gruel J, Girke T, Jönsson H, Reddy GV (2011) WUSCHEL protein movement mediates stem cell homeostasis in the *Arabidopsis* shoot apex. Genes Dev 25:2025–2030

Zhang X, Bernatavichute YV, Cokus S, Pellegrini M, Jacobsen SE (2009) Genome-wide analysis of mono-, di- and trimethylation of histone H3 lysine 4 in *Arabidopsis thaliana*. Genome Biol 10(6):R62

Zheng B, He H, Zheng Y, Wu W, McCormick S (2014) An ARID domain-containing protein within nuclear bodies is required for sperm cell formation in *Arabidopsis thaliana*. PLoS Genet 10(7):e1004421

Zhou Y, Liu X, Engstrom EM, Nimchuk ZL, Pruneda-Paz JL, Tarr PT, Yan A, Kay SA, Meyerowitz EM (2014) Control of plant stem cell function by conserved interacting transcriptional regulators. Nature 517:377–380

Zhu JK (2009) Active DNA demethylation mediated by DNA glycosylases. Annu Rev Genet 43:143–166

Zhu T, Moschou PN, Alvarez JM, Sohlberg JJ, von Arnold S (2014) *WUSCHEL-RELATED HOMEOBOX 8/9* is important for proper embryo patterning in the gymnosperm Norway spruce. J Exp Bot 65:6543–6552

Zuo J, Niu QW, Frugis G, Chua NH (2002) The *WUSCHEL* gene promotes vegetative-to-embryonic transition in *Arabidopsis*. Plant J 30:349–359